

# Stretchable electrochemical energy storage devices

David G. Mackanic,<sup>a</sup> Ting-Hsiang Chang,  <sup>a</sup> Zhuojun Huang,<sup>b</sup> Yi Cui\*<sup>bc</sup> and Zhenan Bao  \*<sup>a</sup>

The increasingly intimate contact between electronics and the human body necessitates the development of stretchable energy storage devices that can conform and adapt to the skin. As such, the development of stretchable batteries and supercapacitors has received significant attention in recent years. This review provides an overview of the general operating principles of batteries and supercapacitors and the requirements to make these devices stretchable. The following sections provide an in-depth analysis of different strategies to convert the conventionally rigid electrochemical energy storage materials into stretchable form factors. Namely, the strategies of strain engineering, rigid island geometry, fiber-like geometry, and intrinsic stretchability are discussed. A wide range of materials are covered for each strategy, including polymers, metals, and ceramics. By comparing the achieved electrochemical performance and strain capability of these different materials strategies, we allow for a side-by-side comparison of the most promising strategies for enabling stretchable electrochemical energy storage. The final section consists of an outlook for future developments and challenges for stretchable supercapacitors and batteries.

## 1. Introduction

The convenience of modern electronic devices has fueled the increasingly intimate interactions between humans and electronic devices. Nowadays, beyond modern electronics such

as laptops and phones, we also utilize wearable electronic devices such as smartwatches that constantly interact with our bodies. Due to the accessibility and comfort these devices provide to our lives, many believe that future development of electronics should aim for their seamless integration as part of the human body.<sup>1,2</sup>

It is predicted that the next generation of electronic devices will be conformable to human skin and will adopt a soft and stretchable conformation. Previous research has already showcased significant progress in developing various conformable electronic components including stretchable transistors,<sup>3,4</sup>

<sup>a</sup> Department of Chemical Engineering, Stanford University, Shriram Center, 443 Via Ortega, Room 307, Stanford, CA, 94305, USA. E-mail: zbao@stanford.edu

<sup>b</sup> Department of Materials Science and Engineering, Stanford University, 476 Lomita Mall, Stanford, CA, 94305, USA. E-mail: yicui@stanford.edu

<sup>c</sup> Stanford Institute for Materials and Energy Sciences, SLAC National Accelerator Laboratory, 2575 Sand Hill Road, Menlo Park, California 94025, USA



David G. Mackanic

David G. Mackanic is a PhD Candidate in the Chemical Engineering Department of Stanford University. His research focuses on developing polymeric materials for advanced batteries. David is supported by the NSF GRFP and a Stanford Graduate Fellowship. He received his BS in Mechanical Engineering and BA in Chemistry from Virginia Tech.

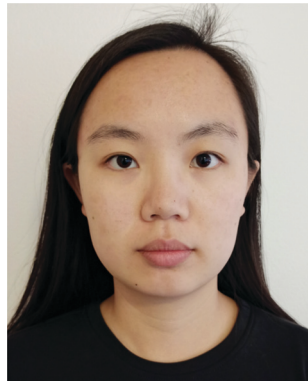


Ting-Hsiang Chang

Ting-Hsiang Chang is currently a visiting postdoctoral research fellow in the Department of Chemical Engineering at Stanford University. He received his PhD in chemical engineering from National Taiwan University. His research interests lie in the development of stretchable electronics and deformable energy storage systems.

displays,<sup>5</sup> sensors,<sup>6–8</sup> and even embedded devices.<sup>9,10</sup> However, the demonstration of integrated stretchable power sources lags behind. To power these conformable devices, we will need to redesign our current energy storage devices to be flexible, stretchable, and conformable to the body. Conventionally, stretchable and conformal electronic devices attempt to mimic the mechanical properties of human skin, which has a modulus of order 1 MPa<sup>11</sup> and experiences strain of ~30%.<sup>12</sup> Applications requiring long-term adherence to the human body or implanted devices may require lower moduli and strain capability of over 100%.<sup>13</sup> Such diverse requirements for various wearable applications highlight the importance of developing robust and tunable methods for making stretchable energy storage devices.

Currently, there are two main types of electrochemical energy storage devices used for powering electronic devices:



**Zhuojun Huang**

*Zhuojun Huang is currently a Materials Science and Engineering PhD student at Stanford University, United States. Her research interests are polymeric materials, energy storage systems and electrochemical reaction interfaces. Zhuojun received her BS from University of California, Berkeley in Materials Science and Engineering.*



**Yi Cui**

*Yi Cui is a Professor in the Department of Materials Science and Engineering at Stanford University. He received BS in Chemistry in 1998 at the University of Science and Technology of China (USTC) and PhD in 2002 at Harvard University. After that, he went on to work as a Miller Postdoctoral Fellow at the University of California, Berkeley. His current research is on nanomaterials for energy storage, photovoltaic, topological insulators,*

*biology and environment. He is a Fellow of Materials Research Society, a Fellow of Royal Society of Chemistry and a Fellow of Electrochemical Society. His selected awards include: Blavatnik National Laureate (2017), MRS Kavli Distinguished Lectureship in Nanoscience (2015), the Sloan Research Fellowship (2010), KAUST Investigator Award (2008), ONR Young Investigator Award (2008), Technology Review World Top Young Innovator Award (2004).*

batteries and supercapacitors. Each of these devices has unique advantages for different applications for wearable electronics. Compared to the different stretchable electronics described above, the creation of stretchable energy storage introduces novel challenges because the stretchability must be enabled on the millimeter scale, compared to thin-film electronics which require active components on the nanometer or micrometer scale.<sup>14</sup> In this review, we discuss recent advances in stretchable battery and supercapacitor technology. Compared to other reviews, we focus on the various strategies that can be taken to make materials and devices stretchable. By showcasing the different methods by which strain capability can be introduced, we hope to provide a roadmap for scientists and engineers to make a wide variety of materials stretchable. All the while, we also document the electrochemical performance of these devices, so that the reader can develop an understanding of what strategies are effective to create materials that are both high performance and highly stretchable.

## 2. Electrochemical energy storage systems

An understanding of the device composition of batteries and supercapacitors is necessary in order to understand how these devices can be engineered into a stretchable form factor.<sup>1,15,16</sup>

Batteries are composed of six main components: anode, cathode, separator, electrolyte, current collector, and encapsulation. During operation, energy is released/stored from the electrochemical reactions at the anode and cathode materials. Within the battery, only ionic transmission between the electrodes is permitted, enabled by an ion conductive electrolyte (Fig. 1a).<sup>17,18</sup>



**Zhenan Bao**

*Zhenan Bao is the K. K. Lee Professor of Chemical Engineering at Stanford University. Prior to joining Stanford in 2004, she was a Distinguished Member of Technical Staff in Bell Labs, Lucent Technologies from 1995–2004. She pioneered a number of design concepts for organic electronic materials. Her work has enabled flexible electronic circuits and displays. In her recent work, she has developed skin-inspired organic electronic materials, which resulted in functions in medical devices, energy storage and environmental applications. Bao is a member of the National Academy of Engineering and the National Academy of Inventors.*

*materials, which resulted in functions in medical devices, energy storage and environmental applications. Bao is a member of the National Academy of Engineering and the National Academy of Inventors.*

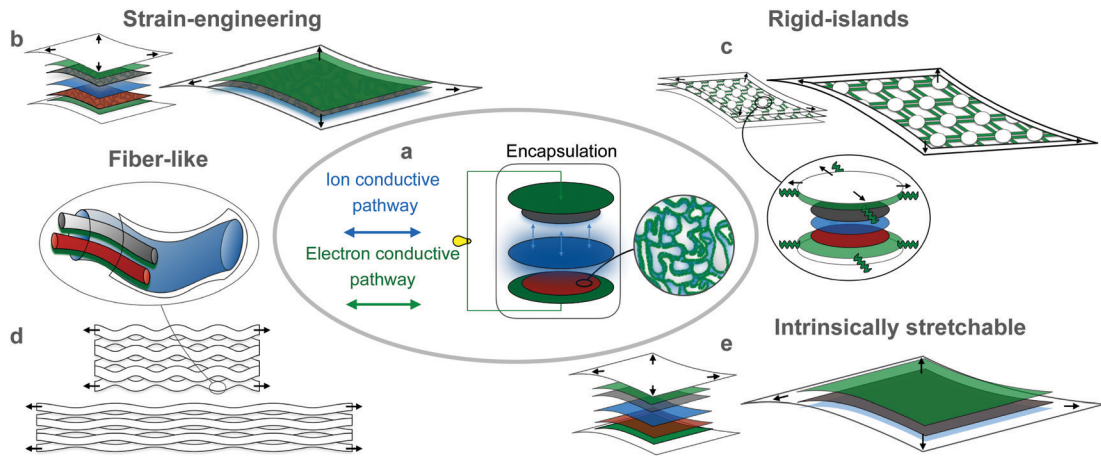


**Fig. 1** Schematics of various electrochemical energy storage device structures: (a) configuration of a conventional rigid battery/supercapacitor with ion conduction pathway (blue shade) and electron conduction route (green shade) marked; structures of stretchable energy storage devices with different mechanisms: anode (red), cathode (dark gray), separator/electrolyte (blue), current collectors (green), encapsulation (white), and stretchable directions (black arrows). Schematics of stretchable devices with (b) microstructured strain-engineering (c) rigid-island (d) fiber-like, and (e) intrinsically stretchable architectures.

The separator is usually made of porous polymeric materials that allows permeation of the electrolyte but prevents the physical contact of the anode and cathode, and thus ensures electronic insulation within the battery.<sup>19</sup> The anode and cathode are only electronically connected *via* an external circuit during operation, where electrons are moved from one electrode to the other as the electrochemical reaction progresses.<sup>20</sup> The only place in the battery where electronic and ionic conduction meet is in the electrodes. Usually, electrodes are active materials mixed with electron conductors such as carbon black and bonded together by polymers such as poly(vinylidene difluoride) (PVDF) that can swell in the electrolyte and enable ionic conduction.<sup>21</sup> Current collectors are usually made of either Al or Cu metals that connect the electrodes to the external circuit. Since many battery components are not only carcinogenic but also sensitive to air and moisture, they are enclosed with robust encapsulation materials, leaving only wires for electronic connections with external circuit.<sup>17</sup> For applications in stretchable electronics that interface with the human body, there is additional motivation to develop non-toxic and safe materials.

The structure of supercapacitors is similar to that of batteries. The primary difference between batteries and supercapacitors is the mechanism of charge storage. The storage mechanism in supercapacitors can be categorized into two different categories – traditional and pseudocapacitive. In a traditional supercapacitor, energy is stored *via* electrostatic polarization of the ions inside the cell, and so the capacity is directly dictated by the surface area of the electrodes.<sup>22</sup> In a pseudocapacitor, energy is stored through facile redox reactions at the electrode–electrolyte interface.<sup>23</sup> Typically, supercapacitors utilize the same structure as batteries but use symmetric electrodes, however asymmetric supercapacitors have also been demonstrated.<sup>24</sup> Between the two electrodes are ion conduction pathway enabled by either liquid or solid electrolytes.<sup>25,26</sup>

## 2.1 Requirements for stretchable energy storage devices

To move from rigid batteries and supercapacitors to stretchable electrochemical energy storage systems, it is not only necessary to reach desirable mechanical properties but also required to maintain all the aforementioned levels of electronic and/or ionic conduction for each component in the device.<sup>1,27</sup> In general, to make a stretchable energy storage device, one needs to develop the following materials in stretchable format: (1) electrodes with both electron and ion conductive pathway; (2) electrolyte and separator that act as ion conductors and electron insulators; (3) current collectors with metal-like electronic conductivity; (4) encapsulation materials that are robust and prevent leakage and gas permeation even under strain.

There are many challenges to achieve the four above mentioned materials. The conventional rigid electrodes in batteries and supercapacitors are rigid granular active materials bound with stiff polymeric binders like PVDF. A simple approach to enable stretchability is to replace the rigid binder with a stretchable one, however the mechanical property mismatch between the rigid active materials and the soft matrix introduces an inherent tradeoff between energy density and stretchability.<sup>28</sup> In a final device, the thickness, mass loading, electron and ion conductivity of the electrode material all must be high to achieve good device performance. It is difficult to develop a strategy that incorporates all of these features. Perhaps most importantly, developing materials that can compete in terms of areal/volumetric energy density is crucial for wearable electronics.

The conventional electrolyte used for electrochemical systems is usually liquid and is thus intrinsically conformable. In many stretchable devices, the liquid electrolyte is coupled together with a polymer matrix to form a gel electrolyte, where the polymer provides mechanical support for the liquid electrolyte and physically separates the anode and cathode. Although the gel-like electrolyte is an effective ion conductor and electron

insulator, encapsulating liquid electrolyte in a stretchable casing has proven to be difficult. The liquid electrolyte can leak to all components of the battery making it difficult to sufficiently seal the device and provide long-term operation. Even if the stretchable devices are successfully encapsulated, the liquid electrolyte may corrode the sealant and cause leakage.<sup>29</sup> Due to the difficulty of encapsulating liquid electrolytes, many have turned to solid-state electrolytes.<sup>30,31</sup> There are two major types of solid electrolytes: ceramic and polymeric. Ceramic solid electrolytes have high ionic conductivity but are rigid and need to be incorporated into an organic matrix for stretchability.<sup>32,33</sup> The interfacial impedance between the ceramic electrolyte and the organic matrix can be hard to overcome and cripple the ionic conductivity of the electrolyte.<sup>34</sup> Alternatively, solid-state polymeric electrolytes are conformal and so do not face the two-phase interfacial impedance challenges that ceramic conductors do. However, the current state of the art polymeric electrolyte has yet to reach the ionic conductive sufficient for room temperature device operation.<sup>35,36</sup> The relatively low ionic conductivity of polymer electrolytes would lead to stretchable storage devices that have low power capability, which is undesirable.<sup>37</sup> Ideally, an electrolyte for deformable energy storage devices would be solid-state with only minor amounts of plasticizer, would be mechanically robust, stretchable, and tough, and would be safe, non-flowable, and non-toxic. Achieving such combination of properties is difficult, but these design principles are important for replacing the conventional separator/electrolyte material.

Current collectors transmit electric currents from inside to outside of the device. Since the electronic conductivity of the current collectors needs to match those of metallic materials, they are usually manufactured *via* deposition of metal onto a stretchable material in the form of a uniform coating or nanostructures.<sup>2</sup> However, the absolute electron conductivity of these conductors is related to the thickness of the metal layer, and while typically thicker metal layers have higher electron conductivity, the stretchability is diminished. Carbon-based materials are also often used, but they typically have lower electronic conductivity than their metallic counterparts.<sup>38</sup> Development of stretchable conductor materials is necessary for devices beyond stretchable batteries, and much existing work is available as a reference to create these soft and stretchable electron conductive materials.<sup>39</sup>

Although commonly overlooked, encapsulation remains one of the most challenging issues for stretchable devices. Currently, most pouch cells utilize a polymeric heat seal material as the packaging, however, this material is flexible but not stretchable.<sup>40</sup> The most commonly used encapsulation material for stretchable energy storage devices is poly(dimethylsiloxane) (PDMS).<sup>1,41</sup> However, the insulating capability of this material is limited, especially under repeated mechanical stress. To overcome this issue, many researchers use a thick PDMS encapsulation layer with a thickness higher than that of active materials in the device stack. Unfortunately, there is a fundamental tradeoff between stretchability and air permeability. The free volume that allows for chain motion and stretchability also typically allows gas permeability.<sup>42</sup> Of existing stretchable

polymer packaging materials, butyl rubber appears to have the lowest air permeability, however the permeability may still be too high for long term operation.<sup>43</sup> Some promising strategies for stretchable encapsulation materials include creating composite structures and creating wavy insulating structures on top of elastomers.<sup>44,45</sup> We have yet to develop an effective insulation material capable of creating oxygen and moisture free environment for device operation even under mechanical strain conditioned.

## 2.2 Cell design considerations

One common device layout for stretchable devices utilizes a planar design, where the anode and cathode are parallel to each other in one plane and embedded in the encapsulation material. Above the electrodes, a layer of electrolyte ionically connects the anode and cathode. A layer of elastomer-embedded metal is coated between the encapsulation and electrode as the current collector and transmits electricity outside of the device. This device structure largely reduces the chances of shorting, since anode and cathode are parallel to each other instead of stacked on top of each other.<sup>27</sup> However, with this configuration, the energy density of the device per surface area is limited, since both encapsulation, cathode, and anode have to fit into one plane. Alternatively, another major device configuration involves the anode, separator/electrolyte and cathode stacked on top of each other. This structure can largely increase the energy density per surface area.<sup>46,47</sup> However, the close distance between anode and cathode, especially under stretching, can cause internal shorting and device failure. When packaging a stretchable device, it is important to consider these tradeoffs and design devices that have both high safety under deformation as well as high energy density.

## 3. General strategies to enable stretchability

As discussed above, the requirements for a fully functional electrochemical energy storage device are manifold. As such, it is unlikely that any one approach to enabling stretchability will suffice for each component of the device. In this review, we have categorized the major strategies to enable strain-capability into 4 broad themes; strain-engineering, rigid island structures, fiber-like structures, and intrinsically stretchable (Fig. 1). In the following section, we provide a high level definition and description of each of these systems.

### 3.1 Strain engineering

While there are different definitions of strain engineering, in this review we use strain engineering to refer any structure that uses a material processing technique to create enhancement in strain capability. This could also refer to using a stretchable substrate to support rigid active materials. Many researchers utilize strain engineering methods where the stretchability derived from changes in materials geometry, and therefore

the requirement for material level stretchability is much lower. Strain engineering can be used for any component of the device. There are various ways on how the anode and cathode are arranged within each strain engineering method, but for simplicity of demonstration, we will use the anode-cathode stack on top of each other geometry to showcase all strain engineering approaches.<sup>1</sup>

One strain engineering approach is to use microstructures, typically *via* either a wavy structure, crumpled structure, or sponge structure. For example molding the device into 3D wave-like structures can largely increase the stretchability. In this mechanism, wavy stretchable devices transform stretching into unbending of the waves, reducing the amount of stress placed on the material itself.<sup>28</sup> Such a technique reduces the requirement for intrinsically stretchable materials and increases the device stability.<sup>1,28,48</sup> One drawback to this technique is that the thickness derived from the wavy structures of this energy storage device can limit its energy density and may provide difficulty when integrated with other electronic components due to the non-planar three-dimensional nature of the waves.

Sponge structures are also a popular strain-engineering choice for building stretchable energy storage devices (Fig. 1b). In this technique, the voids in the sponge plays the same role as previously mentioned wavy structures: redirecting the amount of stress placed on materials to bending torsion. The large surface area of the sponge also allows for the loading of active materials. Usually, a stretchable foam is used as the template and rigid active materials, electron conductors, and binders are infiltrated into the sponge to create the stretchable electrode.<sup>41,49</sup> Since the active materials and the stretchable foam are usually not matched in mechanical strength, if there is not sufficient bonding between the rigid active materials and the sponge template, delamination between the sponge matrix and solid materials can cause capacity fading. Also, the voids in the sponge not filled with active materials reduce the final energy density of the device.

A different technique uses folding patterns based on origami architecture to enable device stretchability. In this method, the strain engineering is in the form of a crease that can fold and unfold to allow a change in the device geometry.<sup>50,51</sup> Once again, although this technique creates devices that are macroscopically stretchable, the materials themselves do not need to be stretchable, only able to accommodate creases at specific location. One drawback to this technique is that the stretchable direction of the device is usually defined by the design of the folds, and so the final device may have anisotropic stretchability.

### 3.2 Rigid island structures

Rigid-island configuration deflects the stress away from rigid components of the device and focuses the stress into stretchable conductive interconnect wires. As shown in Fig. 1c, each rigid island can be regarded as a unit of an electrochemical device with cathode, electrolyte, anode, current collectors and encapsulation stacked among each other.<sup>52-54</sup> The array of islands is electronically connected by spring-like wiring.

These wires themselves are not stretchable, but similar to the microstructured approaches, they utilize specific patterns to allow deformation without the device experiencing strain. Development of such interconnects usually relies on thin serpentine structure, that converts linear strain into bending or buckling strain. Rigid materials, even though not stretchable, can handle a specified amount of bending strain governed by eqn (1).

$$\varepsilon = \left( \frac{d_f + d_s}{2r} \right) \times 100\% \quad (1)$$

where  $\varepsilon$  is the peak strain,  $d_f$  is the thickness of the field,  $d_s$  is the substrate thickness, and  $r$  is the radius of curvature.<sup>55</sup> Following this equation allows for specification of device geometry to accommodate a set amount of strain *via* bending motions. The rigid island method uses many of the same components as current electrochemical systems, but the complication of manufacturing and relatively low weight percentage of active components may cause undue expense to manufacture energy storage devices using this technique.<sup>15</sup>

### 3.3 Fiber-like structures

Fiber-like device structures utilize the matured manufacturing technique, fiber spinning, to fabricate energy storage devices.<sup>16</sup> As shown in Fig. 1d, anode and cathode materials are processed into fibers surrounded by the electrolyte. The final formed fiber is then encapsulated and weaved into fabric. These sort of fiber-like devices are intrinsically flexible because of their cable structure, and the flexible fibers can be used to create a strain-capable fabric by using a pre-defined weaving pattern. Fibers that are directly stretchable can also be created by using helically wound fibers and stretchable substrates/electrolytes.<sup>56</sup> Many stretchable supercapacitors have been made with this method, and the relatively high yield of the device is attributed to the maturity of the fiber spinning industry.<sup>57-60</sup> However, the weight percent of active materials is relatively low compared to electrolyte and encapsulation materials.

### 3.4 Intrinsically stretchable

Intrinsically stretchable devices mean that the components of the device are fully stretchable without relying on any strain engineering, or other techniques (Fig. 1e). The field of intrinsically stretchable devices is relatively nascent compared to the strain engineering, rigid-island, and fiber-like approaches discussed previously. Unlike these techniques, intrinsic stretchability can be difficult to achieve because the stretchability must be embedded into the material system. This can be accomplished either by creating blends of elastomeric active materials, or by creating active materials that are intrinsically stretchable themselves, as has been done in the field of organic semiconductors.<sup>61,62</sup> Furthermore, intrinsically stretchable materials typically involve multiple components, and there is often a tradeoff between the active material loading and the degree of stretchability achieved. However, if they can be realized, intrinsically stretchable devices can have many

distinct advantages including low cost of fabrication and isotropic strain capability.<sup>27</sup>

In the following sections, we review various ways in which each of these approaches for creating stretchable devices have been applied to batteries and supercapacitors.

## 4. Conformal batteries for wearable electronics

Compared to supercapacitors, batteries typically have higher energy density with the tradeoff of having lower power density.<sup>63</sup> In the context of wearable electronics, this would mean that batteries could be preferred where long-term, low power operation is required such as for on-skin sensors. For these applications, stretchable batteries are desirable because of their ability to seamlessly integrate with both the human skin and the device being powered.<sup>64</sup>

The field of stretchable batteries is relatively new, and has seen much exciting progress over the last five years.<sup>65</sup> However the field remains nascent and much work is required to complete to create highly functional, safe, and energy-dense batteries that are stretchable and compliant. Specifically, considerations of cycle life, cost, and performance when subjected to prolonged mechanical abuse are relatively unexplored. This section of the review covers the existing work that has been done to make batteries stretchable through various engineering strategies. As mentioned above, we discuss the strategies of strain-engineering, rigid-islands, fiber-like, and intrinsic stretchability. As a reference point, this section begins with a discussion on flexible batteries, which are a much more developed technology and provide a good guide for the metrics and

considerations that must be considered as the field of stretchable batteries continues to develop.

### 4.1 Flexible batteries

Although on-skin wearable electronics require stretchable components to match the tendency of the human skin to deform in both strain and flexure, flexible electronics offer many advantages compared to conventional rigid electronics for wearable applications.<sup>66–68</sup> To power these flexible electronic devices, researchers have developed many types of flexible batteries.<sup>69–71</sup> The reported flexible batteries have many advantages over traditional commercial batteries, which are rigid and bulky.<sup>72</sup> In addition to being deformable and high performance, flexible batteries allow for the use of novel processing methods that may have advantages for cost or specifically tailored applications.

**4.1.1 High-performance flexible batteries.** At this point, flexible batteries can demonstrate excellent performance that is comparable to the performance of research-scale batteries based on conventional rigid materials. For example, Arias *et al.* reported a flexible LCO/LTO ( $\text{LiCoO}_2/\text{Li}_{4}\text{Ti}_5\text{O}_{12}$ ) battery based on nonwoven fiber electrodes. These non-woven fiber electrodes were easily fabricated by dipping the fibrous mat into an ink containing the active materials (Fig. 2a). The resulting battery had a mass loading of  $1 \text{ mA h cm}^{-2}$  that operated for 450 cycles with 93% capacity retention. Furthermore, the battery demonstrated almost no decay in performance when flexed for one hundred cycles to various radii of curvature.<sup>73</sup> Similarly high performance batteries have been demonstrated in the literature with fabric,<sup>74</sup> CNT,<sup>75–77</sup> paper, or paper substrates.<sup>78,79</sup>

Flexible batteries with advanced battery chemistries have also been demonstrated. These chemistries have improved

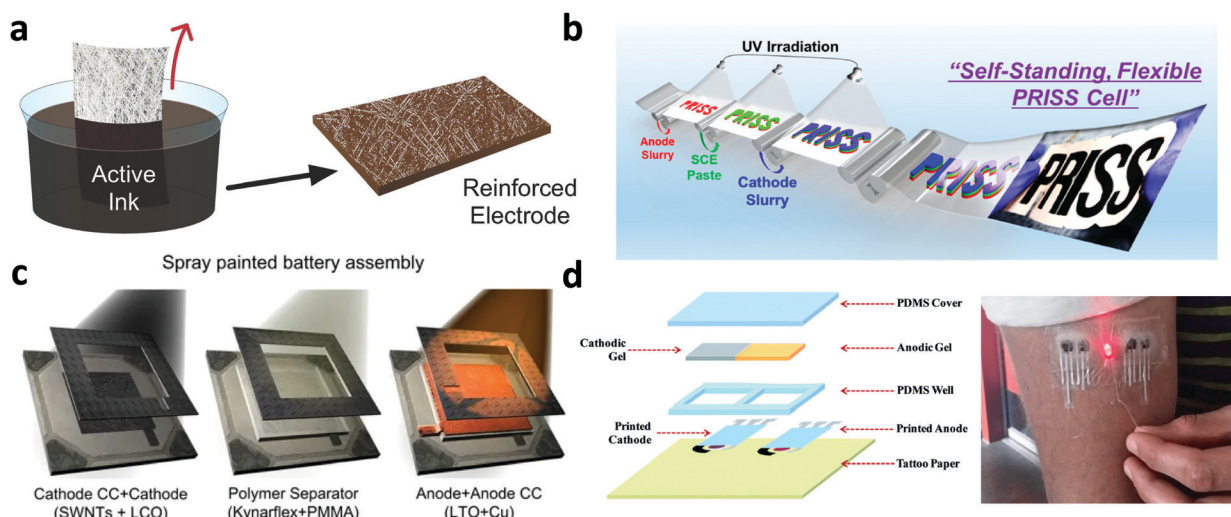


**Fig. 2** Unique fabrication methods and applications of flexible battery technology. (a) Schematic of dip-coating method to create high-performance flexible non-woven fiber electrodes.<sup>73</sup> Reprinted with permission from ref. 73. Copyright 2015 Wiley-VCH. (b) Schematic showing the printing process to create the all-solid-state tri-layer PRISS flexible batteries.<sup>80</sup> Reprinted with permission from ref. 80. Copyright 2015 American Chemical Society. (c) Diagram of a flexible battery fabricated via a spray coating technique.<sup>81</sup> Reprinted with permission from ref. 81. Copyright 2012 Springer Nature. (d) Schematic of an epidermal battery printed on tattoo paper and image showing the battery operating while adhered conformally to human skin.<sup>82</sup> Reprinted with permission from ref. 82. Copyright 2014 Royal Society of Chemistry.

energy density compared to conventional Li-ion batteries while maintaining a stretchable form factor. In one instance, a fiber-like cathode was coated with  $\text{TiO}_2$  nanowires and paired with a lithium metal anode to create a full cell flexible Li–O<sub>2</sub> battery. This battery can operate with gravimetric energy density of over 500 mA h g<sup>−1</sup> even when bent 180° or 360°. Lee *et al.* also demonstrated a high performance flexible battery using a lithium metal anode, with the added advantage of using a solid state ceramic electrolyte.<sup>83</sup> Solid-state batteries are advantageous for wearable batteries because they have enhanced safety compared to conventional batteries with liquid electrolytes.<sup>84</sup> The demonstrated thin-film battery has a low energy density of only  $\sim 0.1$  mA h cm<sup>−2</sup> but has the advantage of being exceptionally thin, which may be useful for various flexible applications. Another research group used a printing process fabricated an all-solid state flexible battery based on a polymer electrolyte (Fig. 2b). These printable solid state (PRISS) batteries demonstrate good performance of an LiFePO<sub>4</sub> (LFP)/LTO battery even when bent tightly around a 5 mm rod.<sup>80</sup>

Another method to improve the safety of batteries is to use an aqueous system as opposed to one that relies on organic liquids. Aqueous batteries are especially desirable for applications in which batteries operate within the human body. Wang *et al.* developed a flexible battery based on symmetric LiVPO<sub>4</sub>F electrodes. The battery uses a high-concentration ‘water-in-salt’ electrolyte which enables a high operation voltage of 2.4 V. This battery demonstrated impressive energy density of 141 W h kg<sup>−1</sup> and could operate at a bending angle of 180° and when cut.<sup>85</sup>

**4.1.2 Unique fabrication methods.** The form factor of flexible batteries allows for the use of unique fabrication methods to create the battery cells. Fabrication methods such as printing, blade coating, printing, and painting have advantages of being low-cost, scalable, and highly tunable.<sup>86,87</sup>

One unique fabrication method used to create flexible batteries involves spray-painting each component of the battery onto a flexible substrate as shown in Fig. 2c. Ajayan *et al.* created a spray-painted LCO/LTO battery where the current collectors, electrodes, and separators were spray painted in separate layers and then packaged in a flexible packaging. The final device demonstrates impressive capacity of 1.2 mA h cm<sup>−2</sup> and was shown to operate in a variety of flexed states.<sup>81</sup>

Another unique fabrication method was reported in the form of a printed tattoo battery. This battery was fabricated by screen-printing current collectors and active materials directly onto tattoo paper (Fig. 2d). Then, a polymer gel electrolyte was injected and the tattoo was encapsulated in PDMS. This battery has a capacity of 1.2 mA h cm<sup>−2</sup> which decreases to 66% of its original value after 100 bending cycles to 180°. Furthermore, this battery demonstrates limited stretchability, although when stretched to only 11% strain, the batteries capacity is reduced to 18% of the initial value.<sup>82</sup> The tattoo battery can be applied conformally and comfortably to the skin, which is likely due to its soft, flexible, and slightly stretchable nature.

This brief summary of flexible batteries sets a reference point for the future work that should be conducted on the next

generation of stretchable batteries. Although flexible batteries are well developed in terms of their performance, chemistry, and processing methods, there are still some milestones that still need to be achieved. Flexible batteries still need to demonstrate energy density on the cell level that is competitive with conventional batteries.<sup>88</sup> For example, most flexible batteries are shown with just a single layer, but commercial LIBs have several stacks of cells in a single packaging. Additionally, flexible batteries should be used to show long-term performance and integration with wearable electronics. The current progress of flexible batteries and the future goals of the technology serve as important benchmarks for the stretchable battery community to meet. Beyond the primary goals of high energy density and deformability, it is also important to consider how advanced chemistries and manufacturing processes can be integrated to create practical commercial devices.

## 4.2 Stretchable batteries

For skin-conformal and human-facing applications of electronics, stretchable batteries are an excellent option for a power source because they can accommodate strain in addition to flexure. While previous reviews have covered stretchable batteries,<sup>1,65,89–91</sup> these reviews primarily focus on material and device-level performance without much description of different strategies of stretchability. In this section, we conduct in-depth analysis of the different methods by which battery materials can be made stretchable. The four major categories are strain engineering, rigid islands, fiber-like, and intrinsically stretchable. Discussing stretchable batteries in this manner is useful to help researchers distinguish the pros and cons of each strategy and to help brainstorm what method to use when trying to make new forms of stretchable battery materials. Descriptions of various stretchable batteries, categorized by the strategy used to make stretchable is provided in Table 1. Some flexible batteries are also included in Table 1 to provide a performance comparison.

**4.2.1 Strain-engineered stretchable batteries.** We categorize strain-engineered stretchability as any material that relies on some form of shape modification to impart stretchability. In the field of stretchable batteries, the main forms of strain engineering used are wavy structure, microstructure, and folded.

**4.2.1.1 Wavy stretchable batteries.** Batteries based on wavy structures have been reported at both the device level and the material level. At the material level, Peng *et al.* demonstrated a novel arched electrode structure that was fabricated by transferring CNTs to a pre-strained PDMS substrate and then releasing the strained PDMS (Fig. 3a and b). The resulting electrodes exhibited high performance due to the excellent conductivity of the CNTs and can handle large strain capability of up to 400%. By combining this unique electrode structure with a stretchable gel electrolyte, the authors were able to create a device that functions at 400% strain with only minor reduction in capacity (Fig. 3c).<sup>92</sup> While this battery demonstrates good strain performance, the mass loading is relatively low at 0.12 mA h cm<sup>−2</sup>. However, the arched CNT electrode

Table 1 Summary of different stretchable batteries reported in literature

Ref.	Chemistry	Electrolyte	Full-cell stretchability (%)	$C/C_0^a$ @ max strain	Strain cycles@ max strain	$C/C_0^a$ post cycles	Loading (mA h cm <sup>-2</sup> )	Discharge voltage	Mechanism of stretchability	Level of stretchability
Strain-engineering										
92	LiMn <sub>2</sub> O <sub>4</sub> /LTO	SCN/LiTFSI-PEO gel	400	0.99	200@400%	0.97	0.12	1.55	Wavy structure	Full device
93	LCO/Graphite	EC/DEC/LiPF <sub>6</sub> liquid	50	0.91	60@50%	0.85	2.2	3.6	Wavy structure	Full device
94	Zn/MnO <sub>2</sub> primary	KOH/ZnO-PAA hydrogel	100	~1	n.r.	n.r.	3.78	1.25	Microstructure fabric	Full device
95	LiFP/LTO	EC/PC/LiPF <sub>6</sub> liquid	100	0.85	n.r.	n.r.	0.165	1	Microstructure, NIPS	Full device
96	LiMn <sub>2</sub> O <sub>4</sub> /Polyimide	Li <sub>2</sub> SO <sub>4</sub> aqueous	100	0.8	n.r.	n.r.	0.045	0.95	Microstructure, breath figure	Full device
97	Si	EC/DEC/LiPF <sub>6</sub> liquid	46	n.r.	1000@25%	1	0.86	0.1	Microstructure, sponge	Anode only
98	LiFP/LTO	EC/DEC/LiPF <sub>6</sub> liquid	80	0.75	500@80%	0.82	1.04	1.8	Microstructure, sponge	Electrodes
99	Na-Ion	PC/FEC/NaClO <sub>4</sub> -PVDF-HFP) gel	50	0.88	100@50%	0.89	~0.6	2.6	Microstructure, sponge	Full device
100	Zn/MnO <sub>2</sub>	KOH/ZnO-PAA gel	100	0.69	n.r.	n.r.	3.6	0.85	Microstructured electrodes	Full device
101	Zn/Ag <sub>2</sub> O	NaOH aqueous	80	0.82	n.r.	n.r.	0.11	1.5	Nanostructured electrodes	Full device
43	LFP/LTO	PVDF-HFP gel	50	0.94	500@50%	0.93	5.1	1.8	Honeycomb microstructure	Full device
102	LCO/LTO	EC/DMC/DEC/LiPF <sub>6</sub> liquid	1300	~1	50@1300%	~1	0.2	2.6	Origami folding	Full device
51	LCO/Graphite	EC/DMC/DEC/LiPF <sub>6</sub> liquid	150	~1	100@83%	n.r.	5.8	3.6	Kirigami folding	Full device
Rigid-island										
103	LCO/LTO	EC/DMC/LiClO <sub>4</sub> -PEO gel	300	n.r.	n.r.	1.15	2.3	Rigid islands	Full device	
104	Li metal	DOL/DMC/LiTFSI) liquid	60	n.r.	100@60%	0.99	1	n.a.	Anode only	Full device
105	Li-air	SCN/LiTFSI-P(VDF-HFP)/PEO gel	100	n.r.	1000@75%	n.r.	2	Rigid islands + wavy structure	Full device	
106	LiCO/graphite	EC/DEC/LiPF <sub>6</sub> liquid	22	0.99	10 <sup>3</sup> @22%	1.01	0.96	3.6	Rigid islands (accordion)	Full device
Fiber-like										
107	LiMn <sub>2</sub> O <sub>4</sub> /LTO	SCN/LiTFSI-PEO gel	100	0.9	200@100%	0.84	n.r.	2.2	Wire shaped	Full device
108	LiMn <sub>2</sub> O <sub>4</sub> /LTO	SCN/LiTFSI-PEO gel	600	0.88	100@100%	0.9	n.r.	2.2	Wire shaped	Full device
109	LiMn <sub>2</sub> O <sub>4</sub> /LTO	SCN/LiTFSI-PEO gel	100	0.85	300@50%	0.99	n.r.	2.5	Wire shaped	Full device
110	Zn/Ag <sub>2</sub> O	KOH/ZnO/Bi <sub>2</sub> O <sub>3</sub> -PAA hydrogel	100	~1	500@100%	1	3.5	1.52	Wire shaped	Full device
111	Al-air	KOH/ZnO/Na <sub>2</sub> SnO <sub>3</sub> -PVA/PEO hydrogel	30	n.r.	n.r.	n.r.	n.r.	1.3	Wire shaped	Full device
Intrinsically stretchable										
112	Zn/MnO <sub>2</sub>	NH <sub>4</sub> /ZnCl <sub>2</sub> -xantham hydrogel	50	0.89	n.r.	n.r.	3.5	1.25	Flowable electrodes	Full device
46	Zn/MnO <sub>2</sub>	KOH-CMC hydrogel	75	~1	700@25%	n.r.	1.44	1.2	Flowable electrodes	Full device
113	EGaIn/MnO <sub>2</sub>	KOH/LiOH-PAAm hydrogel	100	1.25	n.r.	n.r.	3.8	1.47	Flowable electrodes	Full device
114	Zn/Ag <sub>2</sub> O	Aqueous liquid	100	0.83	10@100%	0.83	2.5	1.31	Intrinsic	Full device
115	LFP/LTO	Organic liquid	80	0.96	100@80%	0.95	0.85	1.8	Intrinsic	Electrode only
27	LFP/LTO	DEGDME/LiTFSI-SLIC plasticized polymer	70	0.92	50@50%	0.86	1.1	1.8	Intrinsic	Full device
116	LiMn <sub>2</sub> O <sub>4</sub> /Polyimide	Li <sub>2</sub> SO <sub>4</sub> liquid	30	0.76	30@30%	0.96	0.05	1.25	Intrinsic	Full device
117	LiMn <sub>2</sub> O <sub>4</sub> /e-Li <sub>x</sub> V <sub>2</sub> O <sub>5</sub>	LiTFSI-PAAm crosslinked hydrogel	50	0.65	n.r.	0.056	1	1	Intrinsic	Full device
Flexible batteries										
118	Zn/MnO <sub>2</sub> primary	ZnCl <sub>2</sub>	n.a. <sup>c</sup>	n.a.	n.a.	n.a.	1.1	1.6	Commercial flexible	Full device
119	Li-polymer	Polymer electrolyte	n.a.	n.a.	n.a.	n.a.	~2	3.6	Commercial flexible	Full device
73	LCO/LTO	EC/DEC/LiPF <sub>6</sub> liquid	n.a.	n.a.	n.a.	n.a.	1	2.2	Nonwoven fiber flexible electrodes	Full device
83	LCO/Li	LiPON ceramic	n.a.	n.a.	n.a.	n.a.	0.1	3.9	Thin film flexible	Full device
80	LiFP/LTO	EC/PC/LiPF <sub>6</sub> -ETPTA gel	n.a.	n.a.	n.a.	n.a.	n.r.	1.8	Composite polymer electrode	Full device
81	LCO/LTO	EC/DEC/LiPF <sub>6</sub> -PMMA gel	n.a.	n.a.	n.a.	n.a.	1.2	2.2	Spray-painted on flexible substrate	Full device
82	Zn/Ag <sub>2</sub> O	KOH/LiOH-PAA hydrogel	11	0.18	n.r.	n.r.	1.2	1.5	Printed tattoo paper battery	Full device

<sup>a</sup>  $C/C_0$  refers to the capacity retention of the battery either at the max strain or after the strain cycling. <sup>b</sup> n.r. = not reported. <sup>c</sup> n.a. = not applicable.

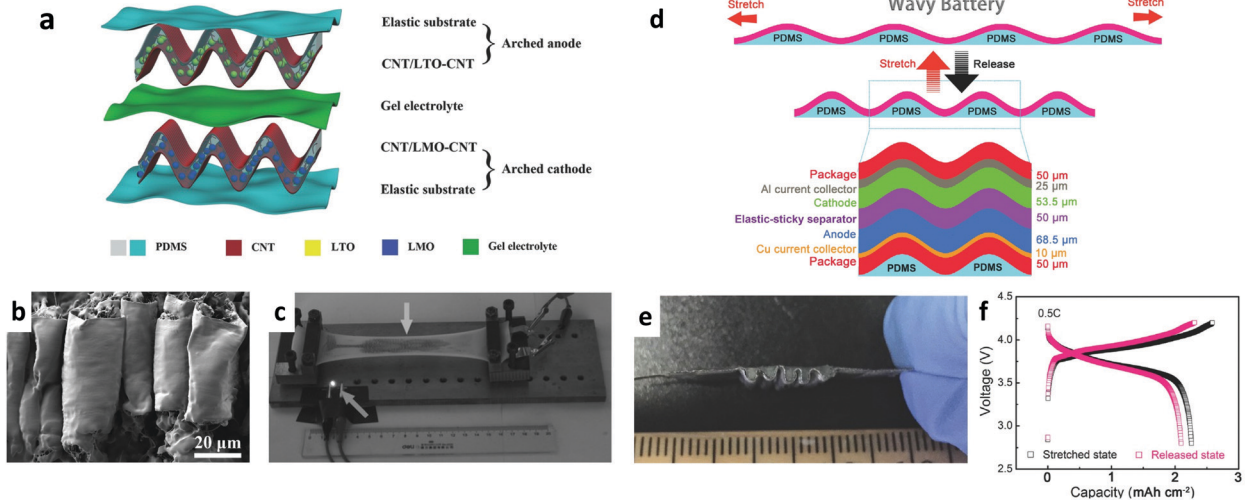


Fig. 3 Two methods of fabricating wavy batteries. (a) Diagram of a stretchable battery based on wavy CNT electrodes fabricated via a pre-straining processes. (b) SEM image of the wavy-structure CNT electrode sheets. (c) Stretchable LIB based on wavy CNT electrode operating at 400% strain.<sup>92</sup> Reprinted with permission from ref. 92. Copyright 2015 Wiley-VCH. (d) Schematic of the wavy-microstructure battery using device-level engineering. (e) Optical image of the wavy battery with PDMS filled in between the wrinkles. (f) Charge-discharge performance of the wavy battery operating at the unstrained and 50% strained state.<sup>93</sup> Reprinted with permission from ref. 93. Copyright 2017 Wiley-VCH.

structure used in this work could be applied to other battery materials as well.

To improve the energy density of the wavy battery structure, Liu *et al.* created a battery that is wavy at the device level (Fig. 3d and e). In this work, commercial cathode and anode materials were used (LCO and graphite) along with a stretchable separator based on electrospun polyurethane (PU)/PVDF. The separator allows for high ionic conductivity when filled with liquid electrolyte, and can also be stretched due to the elastic nature of PU. To make the entire battery stretchable, the packaged battery was molded into a wavy shape and PDMS was used to provide elasticity. The entire battery stack stays well-adhered even during the deformation process due to the sticky nature of the PU/PVDF separator. The results is a stretchable battery with an impressive mass loading of  $3.6 \text{ mA h cm}^{-2}$  and strain capability up to 50% (Fig. 3f).<sup>93</sup>

**4.2.1.2 Microstructure.** This category of material involves a battery electrode that introduces a unique porous geometry through either micro- or nano-structuring to enable strain. Typically, this microstructured substrate is then coated with conventional rigid electrode materials to impart stretchability.

One commercially common way to create a stretchable microstructure is based on weaving thin threads into a fabric. In this way, the stretchability of the knit fabric is higher than the individual fibers.<sup>120</sup> In one of the early examples of stretchable batteries, Steingart *et al.* used a silver-coated woven fabric as a stretchable current collector that was then embedded with Zn and MnO<sub>2</sub> active materials through a dip coating process. The battery demonstrated high mass loading of  $\sim 3.8 \text{ mA h cm}^{-2}$  that was virtually unchanged even when stretched to 100% strain.<sup>94</sup> The use of a commercial woven fabric is advantageous from a processability and scale-up perspective. Despite the

excellent mass loading and high stretchability of the Ag-fabric system demonstrated in this work, relatively little follow up regarding stretchable fabric batteries has been done. In another work, it was found that the silver fabric could be applied to create stretchable LiCoO<sub>2</sub> electrodes with low resistance and a high mass loading of  $22 \text{ mg cm}^{-2}$ . Even though such a cell has a theoretical capacity of nearly  $3 \text{ mA h cm}^{-2}$ , the authors only achieved a capacity of  $0.14 \text{ mA h cm}^{-2}$ . Additionally, a full stretchable battery was not demonstrated.<sup>121</sup> Indeed, stretchable fabric batteries may be an interesting direction for future research effort.

In another work, a stretchable separator membrane was fabricated using nonsolvent-induced phase separation (NIPS). In this technique, an SBS polymer was cast in a good solvent followed by immersion in a nonsolvent, causing liquid-liquid phase separation and the formation of a porous membrane (Fig. 4a). The porosity, and stretchability of these separator membranes could be tuned by varying the concentration of the polymer in the initial solution. By reducing the concentration of the polymer in the initial solution, the stretchability decreased from 450% to 290%, while the porosity increased from 35% to 61% (Fig. 4b and c).<sup>95</sup> This tunability allowed for optimization of a separator that allows for good ion transport *via* liquid electrolyte as well as good stretchability. The same group used a similar method to create a stretchable current collector based on a CNT/carbon black (CB)/PDMS composite. Typically, the inclusion of fillers in PDMS reduces the stretchability dramatically. To create a stretchable carbonaceous PDMS current collector, the group used a breath figure (BF) process which involves evaporating the casting solution in a humidity chamber (Fig. 4d). The BF process allows for the creation of a high-surface area, porous, and elastomeric current collector that contains a large amount of CNT/CB (20 wt% total)

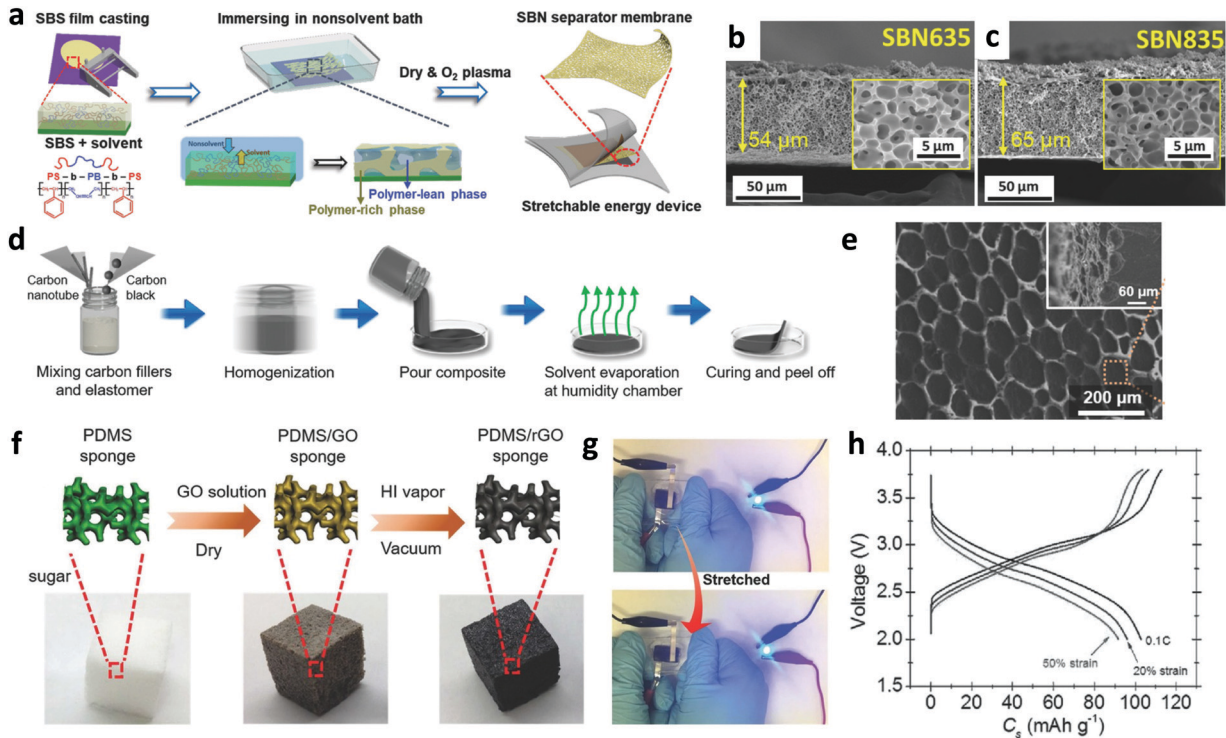


**Fig. 4** Strategies to create microstructured stretchable battery components. (a) Diagram of the NIPS strategy used to create a stretchable porous separator membrane. (b and c) Images showing different porosity of the resulting membranes as a function of the initial polymer concentration in solution.<sup>95</sup> Reprinted with permission from ref. 95. Copyright 2018 Wiley-VCH. (d) Fabrication process to create a porous stretchable current collector via a 'breath figure' method. (e) Resulting porous composite that possesses electronic conductivity and can be loaded with active materials.<sup>96</sup> Reprinted with permission from ref. 96. Copyright 2018 Wiley-VCH. (f) Schematic of the fabrication of 'sponge-like' electrode materials for stretchable batteries. (g) Full cell all-stretchable component sodium ion battery operating at the unstretched and at 50% strain. (h) Charge-discharge curves of the stretchable sodium ion battery at different strain states.<sup>99</sup> Reprinted with permission from ref. 99. Copyright 2017 Wiley-VCH.

and that can be stretched to 200% (Fig. 4e).<sup>96</sup> This unique microstructured current collector allowed for the fabrication of a stretchable aqueous battery that could be stretched to 100% strain. However, despite the use of the high surface area current collector, the mass loading is still low at  $0.045 \text{ mA h cm}^{-2}$ .

One common method of using a porous microstructure to create stretchable batteries is to create 3D sponge structures that are stretchable and have high surface area. One example of this structure is given by Sun *et al.* where a high energy-density rigid silicon sponge is made stretchable by impregnating with a self-healing elastic polymer. While respectable mass loading of  $0.86 \text{ mA h cm}^{-2}$  is achieved with this design, the stretchability is limited due to the rigid nature of the underlying sponge.<sup>97</sup> An improvement of this design involves using an elastic sponge that is coated with active material. Cui *et al.* showed this concept by generating a stretchable porous sponge by templating sugar cubes with PDMS and subsequently removing the sugar. The porous sponge both enables stretchability and has high surface area in which to load active materials. Using this elastic porous scaffold, electrodes with high mass loading of  $14 \text{ mg cm}^{-2}$  were created by slurry casting into the sponges.<sup>98</sup> The LFP/LTO electrodes could also be stretched 500 times to 80% strain while maintaining 82% of their original capacity. While these sponge electrodes have high performance, a stretchable full cell was not demonstrated.

A similar sugar-templated PDMS sponge was used as a microstructured electrolyte by Yu *et al.* for a sodium-ion battery (Fig. 4f). In this case, the use of the sponge was improved by first coating the 3D material with rGO so that the sponge could serve as both a stretchable scaffold and an electronically conductive current collector.<sup>99</sup> After slurry coating VOPO<sub>4</sub> and hard carbon active materials into the stretchable current collector, a mass loading of  $\sim 0.6 \text{ mA h cm}^{-2}$  was achieved with a voltage of 2.6 V. Furthermore, a full cell battery with stretchability of 50% was achieved (Fig. 4g and h). This strategy was also used by another group to create a sponge-like stretchable Li-ion battery.<sup>122</sup> A microstructured sponge electrode was also demonstrated by using an AgNW coated PU foam as the current collector. Then, active materials of Zn and MnO<sub>2</sub> were infiltrated using a dip-coating method. The dip coating of the 3D conductive porous sponge allowed for high active material loading of  $3.6 \text{ mA h cm}^{-2}$  while still achieving a full-cell battery with 100% strain capability with 69% capacity retention.<sup>100</sup>

Another unique microstructure used to create stretchable batteries is the honeycomb structure. In this method, vertically aligned microchannels are crumpled in order to create a strain-capable reentrant structure out of rigid materials. Son *et al.* used graphene, CNTs, and LFP/LTO active materials to create stretchable honeycomb structure batteries. The structures do not require any binder or current collector, allowing for a high

mass loading of  $5.1 \text{ mA h cm}^{-2}$ . This structure also showed very little performance degradation upon stretching, allowing 500 cycles of 50% strain to be obtained with only a 7% decrease in battery capacity.<sup>43</sup> Overall, this honeycomb strategy is promising to achieve high areal capacity, but the low density of the resulting porous electrodes may compromise the overall volumetric capacity.

**4.2.1.3 Folding batteries.** As opposed to engineering wavy structures or micro-structures, nominally stretchable batteries can be fabricated using folding of planar structures. In this case, the components of the battery must be flexible instead of stretchable, but the entire device has the ability to accommodate strain in the form of folding and unfolding. In this way, the strain capability of the battery is discontinuous and geometrically constrained. One well-known example of a foldable battery is the origami battery demonstrated by Jiang *et al.* In this work, a foldable LCO/LTO battery is created by slurry-casting conventional electrode materials into a CNT-coated Kimwipe current collector. After encapsulating the battery, the entire sheet is folded using the Miura folding pattern containing periodic identical parallelograms.<sup>102</sup> This device can reach nominal strains of 1300%, but strain capability that is dependent on folding may not integrate well with existing wearable electronics. Another work by Chan *et al.* also demonstrated the effectiveness of the CNT-based Miura folding batteries.<sup>123</sup>

An advance in the folding approach of stretchable batteries was made by using kirigami folding, which is a method of folding and cutting that allows for the resulting shape to stretch while maintaining a planar geometry. Maintaining a flat geometry while stretching is important because it is more easily integrable with wearable electronics compared to the island and valley structures that emerge when folding and unfolding origami batteries. The kirigami battery was demonstrated to have high capacity of 80 mA h and could be folded to relatively small dimensions of  $5.1 \text{ cm} \times 2.7 \text{ cm} \times 0.26 \text{ cm}$  and stretched to 150% strain.<sup>51</sup> Furthermore, the battery was integrated into a wristband and used to power a smart watch. Such foldable batteries show good performance, but may not be suitable for some applications where intimate contact with the human skin is required. For these applications, continuous stretching along three axis is likely required.

**4.2.2 Rigid island stretchable batteries.** Another strategy for making stretchable devices is using a rigid-island structure. In this strategy, the device consists of islands of rigid active materials that are interconnected by electronically conductive materials that can accommodate strain.<sup>124</sup> While the rigid-island structure could be considered a subset of strain engineering, it is unique in the fact that the device is delineated specifically into two regions – regions that experience strain and regions that do not. The previous section on microstructured materials for stretchable batteries generally do not have strain defined in specific regions.

A well-known example of a rigid island battery was demonstrated by Rogers *et al.* In this work, the rigid islands are circles

of the conventional active materials LCO and LTO on Cu and Al current collectors (Fig. 5a). To enable stretchability, these rigid circles are connected using self-similar serpentine interconnects of the current collector metals (Fig. 5b and c). Even though these metals themselves are not stretchable, the self-similar serpentine structure enables stretchability as the fractal metal patterns bend. Elasticity is imparted to the structure by encapsulating the rigid-island structure in PDMS.<sup>103</sup> The resulting battery has an impressive mass loading of  $1.15 \text{ mA h cm}^{-2}$  and can be stretched biaxially to 300% strain. While the rigid-island structure shown here has excellent battery performance, the use of photolithography methods may be prohibitively expensive compared to traditional slurry-coating process for batteries.

Rigid island structures have also been used to create stretchable battery materials at the component level. Namely, the lithium metal anode is an attractive material for any battery because it has the lowest electrochemical potential and the highest specific capacity.<sup>125,126</sup> However, lithium metal is intrinsically not stretchable. Cui *et al.* demonstrated a stretchable lithium metal anode using 3D micropatterned islands of lithium metal on a copper wire that is stretchable due to an Archimedean spiral geometry (Fig. 5d). The Archimedean coil is encapsulated in styrene–ethylene–butylene–styrene (SEBS) to enable elasticity. The lithium metal anode demonstrates loading of  $1 \text{ mA h cm}^{-2}$  that could be increased with higher amounts of lithium deposition and can be stretched to 60% strain (Fig. 5e and f). A full stretchable battery, however, was not demonstrated.

Another example of a stretchable rigid-island Li metal anode comes from Peng *et al.* In this work, Li metal sheets are laminated onto copper islands that are interconnected with a PDMS-encapsulated elastic copper spring. The rigid lithium islands can then stretch elastically while maintaining electronic connectivity.<sup>105</sup> By combining this rigid island anode with a CNT cathode made stretchable with a wavy microstructure, a functioning Li-air battery was demonstrated. The battery demonstrated a capacity of over  $7000 \text{ mA h g}^{-1}$ , which is quite high. Based on this, a gravimetric energy density of  $2540 \text{ W h kg}^{-1}$  was calculated with strain capability of 100%. Such a high energy density highlights the potential advantages of using high capacity materials such as the lithium metal anode in stretchable batteries.

Another example of a rigid-island type battery is the accordion-like stretchable battery demonstrated by Yang *et al.* This strategy of creating rigid islands is slightly different, in that the rigid islands are full-cell batteries and the serpentine interconnects are created by bending the current collectors in a wavy pattern. The entire device then is encapsulated in a anodized aluminum pouch. The advantage of this method is that it allows for the ‘bellows’ of the accordion to be made of high-energy density stacked layers of active materials.<sup>106</sup> The battery can operate at a variety of bending and stretching states with high performance. A similar battery with a ‘spine-like’ rigid island setup was also demonstrated, but with limited stretchability.<sup>127</sup> Unfortunately, the current designs involves

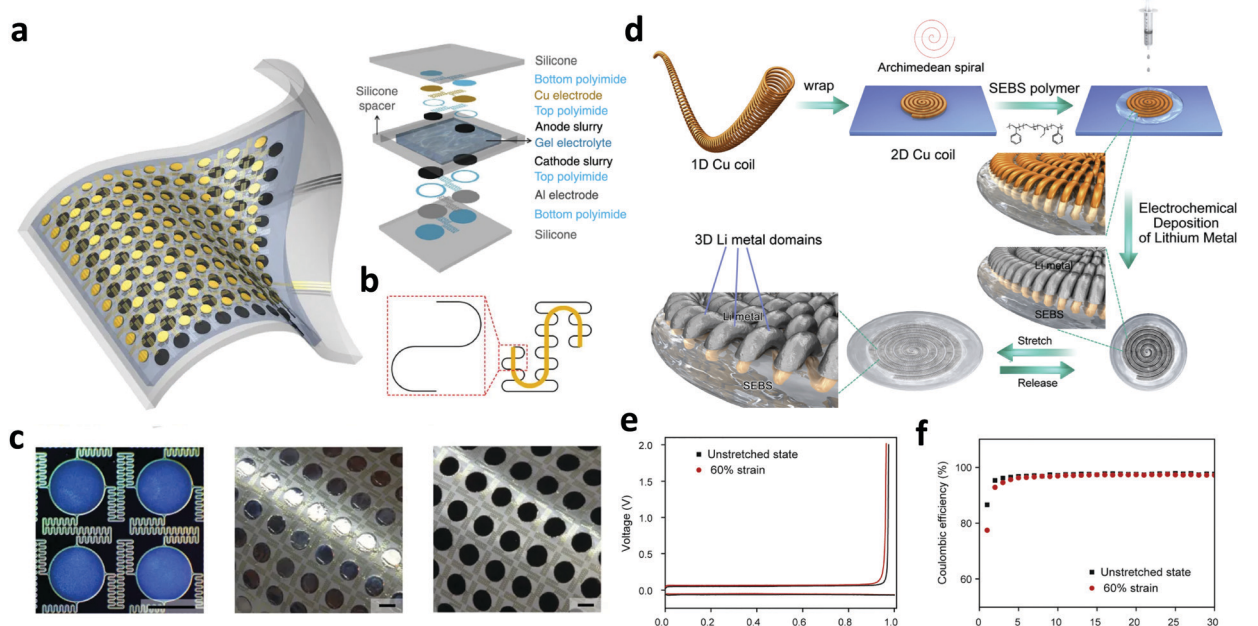


**Fig. 5** Three strategies for fabricating rigid-island batteries. (a) Schematic of the rigid island lithium ion battery fabricated through the use of self-similar serpentine interconnects. (b) Layout of the self-similar serpentine interconnects that allow for the current collectors to stretch without experiencing any strain. (c) Optical images of the rigid-islands connected by the serpentine interconnects.<sup>103</sup> Reprinted with permission from ref. 103. Copyright 2013 Springer Nature. (d) Fabrication process for rigid-islands of lithium metal that can be used as a stretchable anode material. (e and f) Voltage profile and coulombic efficiency for the rigid-island Li-metal anodes operated unstretched and at 60% strain.<sup>104</sup> Reprinted with permission from ref. 104. Copyright 2018 Cell Press.

out-of-plane bending due to the wavy current collectors and also does not appear to be elastic.

**4.2.3 Fiber-like stretchable batteries.** Fiber-like and yarn-like batteries have been covered extensively in other reviews,<sup>128–131</sup> so we do not provide in-depth coverage of all the works in this review. Rather, we aim to highlight select works that showcase the different strategies that can be used to make these fiber-like batteries stretchable.

The first reported fiber-shape stretchable batteries utilized twisted MWCNT yarns that had been immersed in suspensions of LiMn<sub>2</sub>O<sub>4</sub> (LMO)/LTO active materials. These MWCNT yarn composites are not stretchable themselves, but they are mechanically robust and provide excellent charge/discharge performance due to the high conductivity and alignment of the MWCNTs. To create stretchable batteries based on these yarns, they were wrapped around an elastic rod in a helical pattern and coated with a flowable gel electrolyte. When the rod is stretched, the MWCNT yarns simply unwind slightly, causing the fibers themselves to experience little strain. These early fiber-like batteries have relatively low mass loading, but due to the light nature of the CNT yarn supports, the authors estimate that an energy density of 27 W h kg<sup>-1</sup> can be achieved. When considering the mass of the elastic rod in the center of the battery, the achievable energy density is likely lower. The resulting battery can be stretched to 100% strain 200 times with only a 16% decrease in the capacity of the battery.<sup>107</sup> In a follow-on work, the authors demonstrated that they could improve the stretchability of the stretchable batteries by

decreasing the helical angle at which the MWCNT yarns were wrapped around the elastic rod. By essentially winding the yarns closer together around the stretchable substrate, a battery that maintained 88% of its original capacity at 600% strain was achieved. This battery was also demonstrated to be woven into a wristband and a sweater.<sup>108</sup>

One downside of using the MWCNT yarn wrapping approach is that the elastic rod used to enable stretchability is inactive and adds substantial mass compared to the active materials. To overcome this, an alternative design in which the MWCNT yarns form uniform coiled loops. These coiled loops are created by first twisting MWCNT sheets together to form a yarn, and then twisting further to cause the MWCNT yarn to form a spring-like coiled structure. The coiled yarn is demonstrated to stretch reversibly to 100% strain without the presence of an elastic polymer. By coating these coiled fibers in LMO and LTO and then wrapping the electrolyte-coated fibers together, a fiber-like battery with improved energy density and 100% strain capability was demonstrated.<sup>109</sup>

Other chemistries have also been used to create stretchable fiber-like batteries. Zamarayeva *et al.* created a Zn/Ag<sub>2</sub>O battery by sequentially depositing zinc and gel electrolyte onto a spring-like copper current collector and then wrapped the spring like structure with a silver nanoparticle impregnated conductive fabric. By itself, this all-in-one fiber structure is not stretchable, but the authors demonstrated that when the fiber was formed into a serpentine shape and embedded into an elastomer, the battery could be stretched 500 times to 100%

strain with almost no noticeable capacity drop.<sup>110</sup> The authors reported a remarkable areal capacity of  $3.5 \text{ mA h cm}^{-2}$  for this stretchable battery, but this calculation does not include the elastomer-filled area in between the serpentine wire, which makes up the majority of the stretchable device.

Peng *et al.* demonstrated a stretchable fiber-like aluminum air battery through a relatively simple process of coating an aluminum spring with a hydrogel electrolyte and then coating the hydrogel electrolyte with CNT sheets that were coated with AgNPs. The resulting cell is only stretchable to 30%, likely because of the CNT cathode is not microstructured to enhance stretchability. The authors estimated an energy density of  $1168 \text{ W h kg}^{-1}$  for the device, which is well above typical batteries. The Al-air fiber batteries were woven into a wristband and used to power an LED watch. However, Al-air batteries are non-rechargeable, which may limit their use in some applications.<sup>111</sup> Other chemistries have been demonstrated using core-shell stretchable batteries including zinc-air<sup>132</sup> and EGaIn-air.<sup>133</sup>

Overall, fiber-like batteries can be made stretchable, and can have high energy density at the component level. However, since the active material loading in such systems is generally low, it is challenging for such batteries to be scaled up for applications where high volumetric/gravimetric energy density is required.

**4.2.4 Intrinsically stretchable batteries.** The ideal case for stretchable batteries is if they can be made intrinsically stretchable. Relying on strain engineering, rigid-island structures, or fibrous formats may cause for lower overall gravimetric/volumetric energy density because a portion of the battery must be dedicated to the microstructures or inactive interconnects. Additionally, stretchable batteries of such formats typically introduce expensive or complicated fabrication steps, which would likely result in much higher cost compared to typical slurry coating processes used in the battery industry.<sup>134,135</sup> If a stretchable battery could be created using intrinsically stretchable components, the road to commercialization of such a battery would be much more straightforward. In this review, we define intrinsic stretchability as when each component is stretchable in its own right and does not require an elastic substrate or current collector to impart stretchability. Despite the advantages of intrinsically stretchable batteries, relatively little research has been put into this front.

One of the first ever demonstrations of a stretchable battery by Bauer *et al.* in 2010 utilized the concept of intrinsic stretchability. In this work, stretchability is achieved by using liquid-like pastes for the cathode, anode, and current collector (Fig. 6a). The current collector is a carbon black silicon oil paste while the electrode pastes consist of either Zn or  $\text{MnO}_2$  mixed with the either xanthan paste or liquid electrolyte. The battery has high mass loading of  $3.5 \text{ mA h cm}^{-2}$  and can reach strains of up to 50% (Fig. 6b).<sup>112</sup> While liquid pastes are theoretically infinitely stretchable, this work only demonstrates 50% strain due to increasing resistance of the paste components upon stretching. In a follow-on work, the same group demonstrated another stretchable battery using nickel/silver meshes for

the cathode/anode current collectors. These meshes provide high ionic conductivity and stretchability compared to the previous carbon pastes, allowing for the battery to operate at improved strain capability of 75% strain with virtually no capacity fade.<sup>46</sup> The same group also demonstrated a stretchable battery with paste-like electrodes and a crosslinked hydrogel electrolyte, which was able to be integrated into a fully stretchable electronic LED circuit.<sup>136</sup>

Another example of flowable paste-like electrodes was demonstrated by Majidi *et al.* In this work, a unique chemistry involving a liquid metal EGaIn anode and a carbon grease/ $\text{MnO}_2$  cathode were separated by a bilayer hydrogel electrolyte and fixed in place with ecoflex packaging. The stretchability of the cathode was further enhanced by using a pre-strain method prior to depositing the cathode paste on top of the carbon grease. The resulting battery has high mass loading of  $3.8 \text{ mA h cm}^{-2}$  which increases upon stretching to 100% strain due to the increased reaction area of the paste electrodes.<sup>113</sup> It should also be noted that a wide variety of liquid metal anode materials have been explored for battery applications, opening up new opportunities to create high-performance intrinsically stretchable batteries.<sup>137-139</sup> While such paste-based electrodes are interesting because of the ability to accommodate large amounts of strain, they may be undesirable due to large scale flow over long time periods as well as the possibility of leakage.

In an improvement of the ‘electrode paste’ method, Wang *et al.* created a screen printed stretchable Zn/ $\text{Ag}_2\text{O}$  battery by using a hyperelastic binder based on styrene-isoprene-styrene (SIS). With this method, the active materials are mixed directly with the carbon additive and the SIS binder similar to a conventional battery mixing process (Fig. 6c). The use of an elastic binder is an improvement because the electrodes are likely more mechanically robust compared to the previously demonstrated paste-based electrodes. The resulting battery demonstrates impressive strain capability of 100% and high mass loading of  $2.5 \text{ mA h cm}^{-2}$ .<sup>114</sup> However, one disadvantage of this battery is that the power output characteristics and overpotential look very different between the stretched and unstretched states (Fig. 6d), which is undesirable for electronic applications. Another major contribution of this work is the use of screen-printing to create a stretchable battery. Screen-printing is a promising approach to create large-scale flexible battery devices,<sup>140</sup> and has previously been applied successfully in other large-scale flexible/stretchable electronics.<sup>141</sup> Such a facile processing strategy could help to keep the cost of these stretchable batteries low.

A more detailed investigation into the method of using elastomeric binders for stretchable electrodes was conducted by Zhou *et al.* In this work, the elastic binder material poly(styrene)-*b*-poly(*n*-butyl acrylate)-poly(styrene) (SBAS) was used to fabricate an elastic current collector while poly(styrene)-*b*-poly(methyl acrylate)-poly(styrene) (SMAS) was used an elastic electrode binder. The authors used SBAS/SWCNT composites as the current collector and conducted an in-depth investigation of the effect of the conductivity of the current collector on battery performance. They found that a conductivity

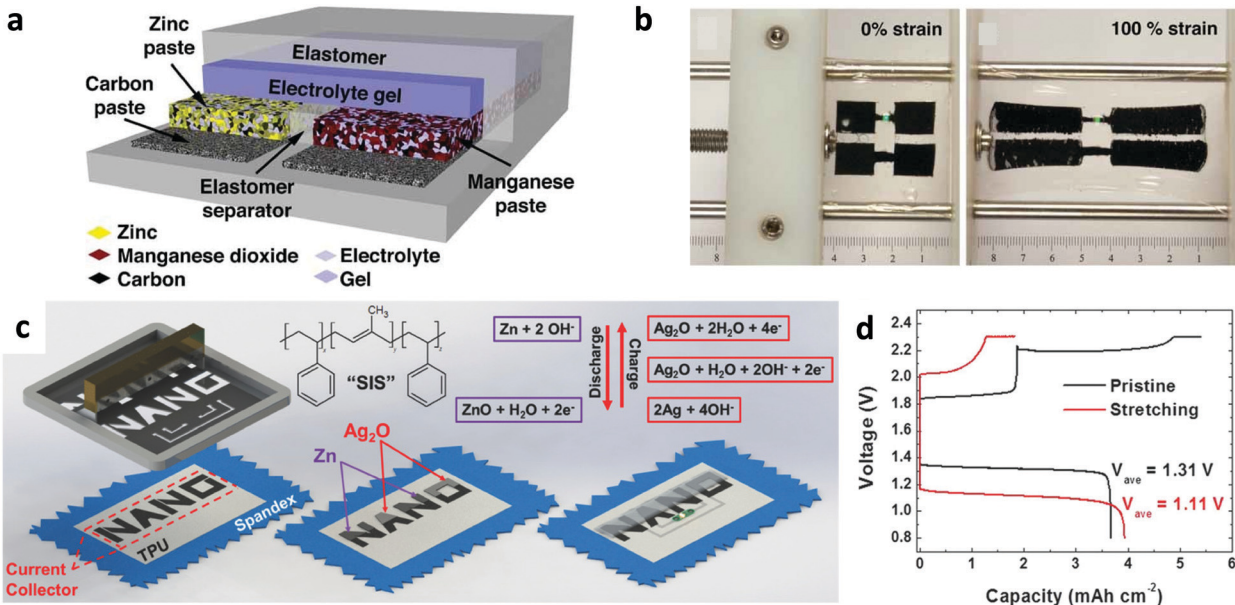


Fig. 6 Intrinsically stretchable batteries using paste or slurry electrodes. (a) Schematic of a stretchable battery using a flowable paste for each component and encapsulated in an elastomer. (b) Image of the battery in (a) powering an LED at 0% and 100% strain states.<sup>112</sup> Reprinted with permission from ref. 112. Copyright 2010 Wiley-VCH. (c) Schematic of the fabrication process for a stretchable battery that creates stretchable electrodes by using a hyperelastic SIS binder. (d) Charge-discharge characteristics of the stretchable battery from (c).<sup>114</sup> Reprinted with permission from ref. 114. Copyright 2017 Wiley-VCH.

of  $10^{-2}$  S cm<sup>-1</sup> is required for effective battery operation. They found that while the SBAS/SWCNT composite with 5 wt% CNT loading could be strained to 100% strain, the electronic conductivity dropped to near  $10^{-3}$  S cm<sup>-1</sup> upon stretching. A 10 wt% composite, on the other hand, could be stretched only to 50% strain before rupture, but maintained high electronic conductivity of  $10^{-2}$  S cm<sup>-1</sup>.<sup>115</sup> This result highlights a fundamental tradeoff for intrinsically stretchable composite active materials; the higher the mass loading of active fillers, the lower the stretchability. Balancing this tradeoff is key to fabricating high-performance intrinsically stretchable batteries. This work also compared the performance of stretchable electrodes with either a PVDF binder compared to an elastic SMAS binder. They found that using an elastic binder of SMAS has higher performance after strain than the PVDF binder due to its ability to accommodate strain. For other works using active materials coated on a microstructured substrate, PVDF is commonly used as a binder. It is likely that these works could demonstrate improved performance if they used stretchable electrodes by replacing PVDF with an elastic binder.

Our recent work reported a good example of the concept of using an ionically conductive elastic binder for stretchable batteries. In this work, a stretchable lithium ion conducting (SLIC) polymer containing poly(propylene oxide)/poly(ethylene oxide) (PPO/PEO) domains and hydrogen bonding 2-ureido-4-pyrimidone (UPy) domains was synthesized (Fig. 7a). When mixed with lithium bis(trifluoromethylsulfonyl)amine (LiTFSI) and 20 wt% diethylene glycol dimethyl ether (DEGDME), this polymer demonstrated high ionic conductivity of  $\sim 2 \times 10^{-4}$  S cm<sup>-1</sup> and extreme toughness of 29.3 MJ m<sup>-3</sup> (Fig. 7b).

We showed that this highly stretchable conductive polymer can be used as an intrinsically stretchable polymer electrolyte as well as a binder material. Intrinsically stretchable composite electrodes were fabricated, and 100% strain capability was achieved with low polymer content of only 20 wt%. Additionally, the fact that the UPy domains were used in both the electrode and electrolyte meant that strong interfaces were formed between the different components of the battery. As a result, a battery with 70% strain capability and impressive mass loading of 1.2 mA h cm<sup>-2</sup> was demonstrated (Fig. 7c and d). Furthermore, the power output characteristics of the battery did not significantly change upon stretching.<sup>27</sup> This work utilized an intrinsically stretchable microcracked gold current collector with low resistance of around  $20 \Omega \square^{-1}$ , however the resistance of the current collector increased upon stretching, ultimately limiting the overall stretchability of the device.

As such, developing intrinsically stretchable current collectors is important to enable stretchable lithium ion batteries. Much work has been conducted on stretchable electronic conductors in general,<sup>39</sup> and a few recent works focus on developing intrinsically stretchable current collectors for batteries. In one notable work, stretchable current collectors for aqueous LiMn<sub>2</sub>O<sub>4</sub>/polyimide batteries were fabricated using gradient assembled polyurethane (GAP). The GAP strategy involves creating multi-layered structures of stretchable PU/AuNP composites (Fig. 7e). It was observed that when the layers had a high gradient of conductive filler between layers (e.g. 90/50/90 wt%), the stretchability could be enhanced from  $\sim 90\%$  to  $\sim 440\%$  while maintaining similar electronic conductivity. The authors also found that increasing the number of high-gradient

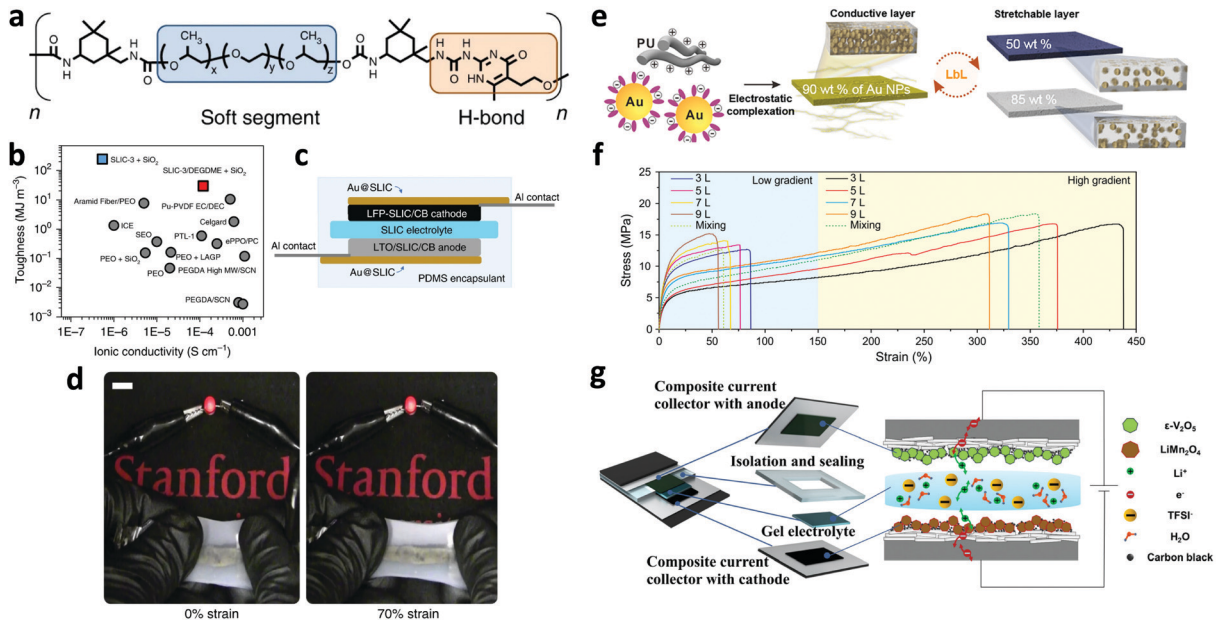


Fig. 7 Intrinsic stretchability of batteries. (a) Chemical structure of the SLIC polymer used as a stretchable electrolyte and current collector. (b) Diagram showing the high performance of the SLIC polymer compared to other polymer electrolytes in terms of ionic conductivity and toughness. (c) Schematic of the stretchable battery created using all SLIC components. (d) Operation of the SLIC battery under various deformation states.<sup>27</sup> Reprinted with permission from ref. 27. Copyright 2019 Springer Nature. (e) Concept of creating a stretchable current collector with various gradient layers of PU/AuNP composites. (f) Effect of different compositions of gradient multilayer conductors on stretchability.<sup>116</sup> Reprinted with permission from ref. 116. Copyright 2019 American Association for the Advancement of Science. (g) Diagram showing the creation of an integrated stretchable battery using a carbon/Ag microflake elastomer composite current collector.<sup>117</sup> Reprinted with permission from ref. 117. Copyright 2019 Wiley-VCH.

PU/AuNP layers in the structure lowered the overall stretchability but increased the through-plane conductivity (Fig. 7f).<sup>116</sup> The stretchable conductors still show increased resistance upon stretching, and so only 30% strain capability of the final battery was demonstrated in this work.

In another example of an intrinsically stretchable current collector, Niederberger *et al.* created an SEBS/CNT/CB/Ag (SCCA) composite in which the carbon materials were mixed with the elastomer directly and silver microflakes were coated on top of the carbon composite. The silver flakes on the surface provide excellent local conductivity while the SEBS/carbon composite provides an electronically conductive pathway to ensure that the electrode remains conductive upon strain. Remarkably, this current collector has a resistance of  $0.53 \Omega \square^{-1}$  at the unstrained state which increases to only  $2.71 \Omega \square^{-1}$  upon stretching to 100% strain. The SEBS/carbon composite without a silver layer, on the other hand increases by a much larger amount, from  $115$  to  $200 \Omega \square^{-1}$ , when stretched to 100% strain. This highlights synergy of the high-conductivity silver surface coating with the stretchable nature of the carbon composite.<sup>117</sup> This study also demonstrated the use of an elastic crosslinked water-in-salt (WIS) electrolyte to create a stretchable battery with 50% strain capability (Fig. 7f). Use of an elastic crosslinked electrolyte helps prevent device shorting.<sup>142</sup> One drawback of the two stretchable current collectors described above is the utilization of a spray coating method to create electrodes, which typically results in low mass loadings.

Overall, each strategy of creating stretchable batteries has distinct pros and cons. While strain-engineering approaches

such as wavy structures, microstructures, and folding can result in high energy density and stretchability, there is often an expensive processing step involved and the use of porous structures can result in lower overall gravimetric or volumetric energy density. A rigid-island approach can provide little degradation in performance upon strain, but the energy density may suffer due to the presence of inactive regions in the battery. Similarly, fiber-like batteries are highly functional and easily integrated into a number of applications, but the overall energy provided may be low due to the small amount of active material in the fiber. Intrinsically stretchable batteries may be able to bridge these tradeoffs, but there is still much research required to create intrinsically stretchable components with acceptable mass loading, electron/ion conductivity, and strain performance. However, based on the study of each of these strategies to create stretchable batteries, there are several guidelines that can be proposed.

(1) The use of an elastomeric binder instead of PVDF can improve the strain performance of electrode materials in stretchable batteries. An elastic, ionically conductive binder should offer additional advantages.

(2) Carbon-based elastomer blends typically have low electronic conductivity, which can be improved by coating with a high-conductivity metal layer.

(3) Gelled polymer electrolytes demonstrate excellent performance in several different stretchable battery applications, and can be more effective if they have elastic characteristics.

(4) Slurry-casting processes can result in higher mass loading than spray-coating processes, and should be pursued if possible.

## 5. Stretchable supercapacitors for wearable electronics

Although batteries are typically favored among power sources for electronic devices due to their superior energy density, supercapacitors have shown great potential for mobile energy storage technology as they possess merits of the high power density, longer cycle life, and fast charging/discharging capability, and ability to bridge the power/energy gap between conventional capacitors and batteries/fuel cells.<sup>143,144</sup> The stretchable supercapacitors are expected to have broad applications in wearable electronics and bio-integrated electronics, especially for those with electronic circuits and components required high power density and high-speed charge/discharge capability. Moreover, the stretchable supercapacitors can be integrated with wearable energy harvesting units such as triboelectric devices and piezoelectric devices to store energy from sporadic body motions, which requires a fast charging rate. On the other hand, compared with lithium-ion batteries, supercapacitors have improved rapidly in recent years due to relatively easier fabrication and structure. In this section, we forego in-depth discussion of the basic information such as electrochemical mechanism (e.g. pseudocapacitance, electrochemical double-layer capacitance), active materials (e.g. carbon-based materials, conducting polymers, and metal oxides), and device configuration (co-facial or planar interdigitated electrodes) for supercapacitors, which have received significant attention in multiple review literature.<sup>25,145,146</sup> Instead, we focus on structural design along with the achieved deformability, stability of electrochemical performances, and practical applications.

### 5.1 Flexible supercapacitors

Flexible supercapacitors have attracted much attention due to their intrinsic advantages for wearable and flexible electronics, such as their small size, lightweight, and mechanical durability, which make them promising flexible energy storage devices.<sup>147</sup> To achieve flexibility, much effort has been devoted to supporting active materials on flexible substrates. Various strategies have been studied for flexible substrates, such as flexible metal substrates,<sup>148–150</sup> carbon-based electrodes,<sup>151–154</sup> paper substrates,<sup>155,156</sup> wire-type/textile electrodes,<sup>157,158</sup> sponge/porous configuration,<sup>159,160</sup> and bendable plastics.<sup>161–163</sup> Each strategy has its advantage and limitation, and no fabrication method is currently dominant in the fabrication of flexible supercapacitors. Thus, we do not provide in-depth coverage of these strategies in this section. Instead, we aim to highlight some interesting achievements on flexible supercapacitors integrated with flexible or stretchable electronics.

The existing integrated flexible systems can be categorized into two types: (i) supercapacitors are utilized as the power source to drive functional devices; (ii) supercapacitors are integrated with energy harvesters. An example of the type (i) is a fiber-based flexible integrated photodetecting system for simultaneous energy supply and optoelectronic detection (Fig. 8a).<sup>164</sup> In this system,  $\text{Co}_3\text{O}_4$  nanowires on nickel fibers served as the positive electrode for supercapacitors; while

graphene acted as both the light-sensitive material for photodetector and the negative electrode for supercapacitors. Another example is a body-attachable and multifunctional system powered by foam-like structure supercapacitors (Fig. 8b).<sup>165</sup> The integrated system consists of flexible supercapacitors, pressure sensor, a strain sensor, and a temperature sensor, and liquid metal interconnections.

Unfortunately, there are no charging components reported in the above-mentioned integrated system, thus the integration of charging systems such as a wireless RF power receiver or energy conversion devices would be helpful to form an all-in-one self-driven integrated system. Fig. 8c shows the schematic illustration of the integrated photo-supercapacitor system. The fiber-like supercapacitor was connected to another fiber-like dye-sensitized solar cell, and the photovoltaic and electrochemical properties were characterized (Fig. 8d and e).<sup>166</sup> The entire photoelectric conversion and storage efficiency was calculated to be about 1.5% by multiplying conversion efficiency (2.2%) and storage efficiency (68.4%). It is envisaged that the fiber structure can be easily integrated into electronic textiles by a well-defined weaving technique and serve as a self-powering system for wearable gadgets.

Despite the numerous efforts devoted to the design and fabrication of flexible supercapacitors, there are still grand challenges hindering the realization of their practical applications. The main challenges include: (i) novel packaging materials and suitable encapsulation technology are crucial for flexible supercapacitors to improve the ability to resist structure and functional failure resulted from repeatable deformations. (ii) The integration of functional devices with flexible supercapacitors is still at a primary level. It would be a very critical topic to pursue integrated circuit design with a smaller device volume for portable and wearable systems. (iii) Development of cost-effective fabrication processes to spin out flexible supercapacitors from lab to commercial products.

### 5.2 Stretchable supercapacitors

One of the key challenges for stretchable energy storage devices is to fabricate reliable electrodes with excellent mechanical and electrochemical stability. Compared with stretchable batteries, the development of stretchable supercapacitors has progressed rapidly due to relative easier fabrication procedures. Creating structures that can be stretched *via* engineering efforts is the most successful strategy for stretchable electrodes. A few different strategies have been presented for designing stretchable supercapacitors, including the wavy-shape design, micro-structure design, rigid island design, kirigami/origami design, fiber-shape design, and textiles design. In this section, we categorize five representative strategies of structural design for the creation of stretchable supercapacitors: (i) buckling stiff active materials into out-of-plane architectures that enable the programmable actuation to mimic stretchability; (ii) micro-structure design with unique pattern and morphology coated with rigid active materials to impart stretchability; (iii) folding design by exploiting predefined crease or cut patterns that can be stretched; (iv) rigid island design combining elastomeric

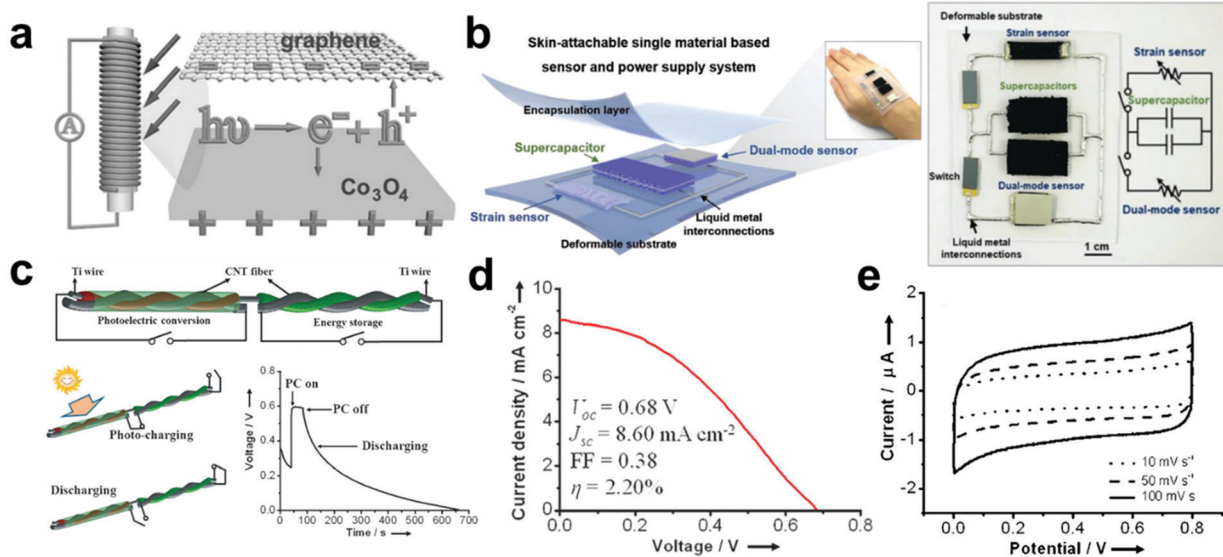


**Fig. 8** Functional electronics integrated with flexible supercapacitors. (a) Schematic illustration of the integrated system. The current response of the photodetector powered by the flexible supercapacitor.<sup>164</sup> Reprinted with permission from ref. 164. Copyright 2014 Wiley-VCH. (b) Multifunctional system powered by supercapacitor with foam structure.<sup>165</sup> Reprinted with permission from ref. 165. Copyright 2018 Wiley-VCH. (c) Wire-shaped device for photoelectric conversion and supercapacitors. Characterization of (d) the photoelectric conversion part and (e) the energy-storage part.<sup>166</sup> Reprinted with permission from ref. 166. Copyright 2012 Wiley-VCH.

bridge and rigid supercapacitors array; (v) fiber, wire, and yarn-shaped design and the advanced textile structures; (vi) towards intrinsically stretchable structures. A variety of stretchable supercapacitor materials are presented in Table 2, with their strain compliance and electrochemical performance documented. Table 2 also includes some examples of flexible supercapacitors to provide a performance comparison.

### 5.2.1 Strain-engineered stretchable supercapacitors

**5.2.1.1 Pre-strain (Wavy/Buckled) design.** One of the simplest strategies for achieving stretchable configuration is the pre-strain method. The key of this strategy is to introduce an initial strain difference in elastomeric substrates and stiff films, either by thermally induced actuation<sup>202</sup> or mechanical prestrain.<sup>203,204</sup> Basically, the active materials were deposited on prestretched elastomeric substrates and wavy structures were formed after releasing the strain (Fig. 9a). The resulting periodically wavy structure rendered the electrodes with certain stretchability. The most commonly used active materials for buckled supercapacitors are carbon-based materials such as CNT and graphene, where the CNT or graphene films served as both electroactive materials and current collectors due to their high surface areas and excellent electrical conductivity. Jiang's group presented a pioneer work on stretchable supercapacitors using this prestrain strategy in 2009, and the electrochemical performance of the as-built supercapacitors remained unchanged under 30% applied tensile strain.<sup>205</sup> A further advance in specific capacity and stretchability was achieved by the integration of accordion-like wavy electrodes and a vinyl hybrid silica nanoparticle reinforced hydrogel polyelectrolyte.<sup>167</sup> By applying the prestrain method with a CNT/poly(pyrrole) (PPy) composite as the electrode, the as-prepared supercapacitor with accordion-like structure could achieve an unprecedented stretchability of 1000% strain with over 2.5 folds

of capacitance improvement due to the increased contact interfaces between electrodes and the electrolyte (Fig. 9b and c).

A further effort on the development of harnessing the interfacial instability to deform the planar films into out-of-plane structures have been devoted in recent years.<sup>206,207</sup> Several different approaches have been developed to achieving complex surface architectures of active materials (e.g., ripples, wrinkles, and crumples) on elastic substrates (e.g., PDMS, Ecoflex, and VHB series). Recently, Cao *et al.* demonstrated a new type of stretchable supercapacitors based on crumpled vertically aligned CNT forests transferred to an elastomer substrate (Fig. 9d).<sup>173</sup> A square-shaped acrylic elastomeric VHB tape was first stretched along with two orthogonal in-plane directions (prestrain 300%  $\times$  300%). The vertical-aligned CNT film was then bonded onto the prestrained elastomer film by a dry transfer method. Relaxing one prestretched direction resulted in unidirectional wrinkles, while biaxial relaxing produced the wrinkles from two dimensions and thus formed crumpled CNT films (Fig. 9e).

Based on the same concept, Chou and co-workers also reported an omnidirectionally stretchable supercapacitor as shown in Fig. 9f. A circle-shaped acrylic elastomer was first isotropically buckled to 200% strain, and the polyaniline (PANI)@CNT film was then deposited onto the pre-strained elastomer substrate. Relaxing pre-stretched direction produced in the wrinkles from omnidirection and thus formed crumpled CNT films. The resulting supercapacitor maintained its electrochemical performance during uniaxial, biaxial, and omnidirectional elongations up to 200% strain with a specific areal capacity of 9.52 mF cm<sup>-2</sup> at a scan rate of 50 mV s<sup>-1</sup>. There are also many other pieces of literature using similar prestrain strategies,<sup>169,171,172</sup> making the prestrain method most popular in preparing stretchable electrodes and supercapacitors.

Table 2 Summary of different stretchable supercapacitors reported in literature

Ref. Materials	Electrolyte	Full-cell stretchability (%)	$C/C_0^a$ @ max strain	Strain cycles	$C/C_0^a$ post strain cycles	Specific capacitance	$C/C_0^a$ post strain cycles	Voltage (V)	Stretchability strategy	Level of stretchability
<b>Strain-engineering</b>										
167 PPy@CNT	$H_3PO_4/VSNP-PAM$ hydrogel	1000	2.6	n.r. <sup>b</sup>	n.r.	200 F g <sup>-1</sup> @10 mV s <sup>-1</sup>	0.6	Buckled way	Symmetric device	
168 PPy@CNT	$H_3PO_4/VSNP-PAA$ hydrogel	600	3.1	n.r.	n.r.	205 F g <sup>-1</sup> @10 mV s <sup>-1</sup>	0.6	Buckled way	Symmetric device	
169 $Fe_2O_3$ (CNT)/ $MnO_2$ /CNT	$Na_2SO_4/PVA$ gel	100	~1	$10^3$ @100%	0.99	82.4 F g <sup>-1</sup> @0.1 A g <sup>-1</sup>	2	Buckled way	Asymmetric device	
170 PANI@CNT	$H_2SO_4/PVA$ gel	200	1.06	$20$ @200%	0.97	1.147 F g <sup>-1</sup> @10 mV s <sup>-1</sup>	0.8	Buckled crumple	Symmetric device	
171 $Ti_3C_2T_x$ /AC	$Li_2SO_4/PVA$ gel	100	0.9	3000@100%	0.93	46 F g <sup>-1</sup> @25 mV s <sup>-1</sup>	1	Buckled crumple	Asymmetric device	
172 Graphene paper	$H_3PO_4/PVA$ gel	Areal 300	0.57	n.r.	49 F g <sup>-1</sup> @1 A g <sup>-1</sup>	1	Buckled crumple	Symmetric device		
173 CNT forest	KCl/PVA gel	Uniaxial 200	1.02	1000@200%	0.96	196 F g <sup>-1</sup> @1 A g <sup>-1</sup>	0-1	Electrode only	Electrode only	
174 Mn/Mo@MWCNT	LiTFSI/ADN/SN/PMMA	Areal 300	0.99	n.r.	2.3 mF cm <sup>-2</sup> @0.1 mA cm <sup>-2</sup>	0.8	Buckled crumple	Symmetric device		
175 RGO microribbons	$H_3PO_4/PVA$ gel	Areal 50	0.94	12000@300%	0.95	17.5 mF cm <sup>-2</sup> @0.1 mA cm <sup>-2</sup>	0-0.8	Microstructured electrode	Electrode only	
176 MWCNT/PANI	PMMA-PC-LiClO <sub>4</sub>	50	n.r.	5000@50%	0.92	1.08 mF cm <sup>-2</sup> @100 mV s <sup>-1</sup>	0.8	Microstructured electrode	Symmetric MSC	
177 SWCNT	$H_3PO_4/PVA$ gel	40	0.9	n.r.	44.1 mF cm <sup>-2</sup> @0.2 mA cm <sup>-2</sup>	3.2	Structured PDMS array	Symmetric MSC		
178 PPy/BPO-CNT	$H_3PO_4/PVA$ gel	150	1.02	n.r.	0.15 F cm <sup>-3</sup> @50 mV s <sup>-1</sup>	3	Honeycomb Structure array	Symmetric MSC		
179 CNT/PANI film	$H_3PO_4/PVA$ gel	2000	~1	$10^3$ @2000%	0.95	7.35 F cm <sup>-2</sup> @7.8 mA cm <sup>-2</sup>	0.24	3D Honeycomb lantern	Symmetric devices in series	
180 $MnO_2/CNT/NCF$ composite	$LiCl/PVA$ gel	140	~1	3000@140%	0.98	72.9 mF cm <sup>-2</sup> @0.5 mA cm <sup>-2</sup>	1	Kirigami	Symmetric device	
181 $Ti_3C_2T_x/BC$ composite	$H_2SO_4/PVA$ gel	400	~1	$10^3$ @400%	0.98	230.5 mF cm <sup>-2</sup> @1.6 mA cm <sup>-2</sup>	0.8	Kirigami	Symmetric device	
182 SWCNT	$H_3PO_4/PVA$ gel	100	~1	5000@100%	0.72	111.5 mF cm <sup>-2</sup> @2 mA cm <sup>-2</sup>	0.6	Kirigami	Symmetric MSC array	
<b>Rigid islands</b>										
183 MWCNT	$[EMIM][NTf_2]/PS-b-PMMA$ ion-gel $[EMIM][TFSI]/PEGDA$ ionogel	30	~0.8	n.r.	n.r.	20.7 F g <sup>-1</sup> @5 A g <sup>-1</sup>	3	Rigid islands-serpentine bridge	Symmetric MSC array	
184 MWCNT/ $Mn_3O_4$	$H_3PO_4/PVA$ gel	Areal 50	0.99	1000@30%	0.96	5 F cm <sup>-3</sup> @6.6 $\mu$ A	6	Rigid islands-liquid metal bridge	Symmetric MSC array	
185 $MnO_2/CNT$	LiCl/PVA gel	Uniaxial	0.99	5000@70%	0.96	5 F cm <sup>-3</sup> @6.6 $\mu$ A	6	Rigid islands-liquid metal bridge	Symmetric MSC array	
186 CNT	$H_3PO_4/PVA$ gel	40	~1	3000@40%	0.92	0.57 mF cm <sup>-2</sup> @10 mV s <sup>-1</sup>	3	Rigid islands-liquid metal bridge	Symmetric MSC array	
187 $MnO_2@CNT//PPy@CNT$	KOH/PVA gel	600	0.9	100@600%	0.97	16.1 mF cm <sup>-2</sup> @10 mV s <sup>-1</sup>	0.8	Buckled Fiber	Symmetric device	
188 pDA-Gr NCA CF	$H_2SO_4/PVA$ gel	75	0.9	1000@75%	0.9	72.9 F g <sup>-1</sup> @0.1 A g <sup>-1</sup>	0.8	Wire shaped	Symmetric device	
189 $MnO_2/CNT$	LiCl/PVA gel	20	0.94	5000@20%	0.8	7.72 F g <sup>-1</sup> @10 mV s <sup>-1</sup>	1.5	Wire shaped	Asymmetric device	
190 CNT/graphene/PANI	$H_3PO_4/PVA$ gel	50	0.95	$10^3$ @50%	0.94	27.5 mF cm <sup>-2</sup> @1.5 mA cm <sup>-2</sup>	0.8	Fiber shaped	Symmetric device	
191 PPy/RGO/MWCNT	$H_3PO_4/PVA$ gel	800	0.97	5000@800%	0.77	137.5 F g <sup>-1</sup> @1 A g <sup>-1</sup>	0.8	Fiber shaped	Symmetric device	
192 $MnO_3/MWCNT$	CAN-PC-PMMA-LiClO <sub>4</sub>	100	0.82	n.r.	7.9 F cm <sup>-3</sup> @0.1 mV s <sup>-1</sup>	0.8	Spring shaped	Symmetric device		
		50	~1	5000@50%	0.8	33.8 mF cm <sup>-2</sup> @0.1 mA cm <sup>-2</sup>	1.4	Textile	Symmetric device	

Table 2 (continued)

Ref. Materials	Electrolyte	Full-cell stretchability (%)	$C/C_0$ @ max strain	Strain cycles	$C/C_0$ <sup>a</sup> post strain cycles	Specific capacitance	Voltage (V)	Stretchability strategy	Level of stretchability
Intrinsically stretchable (embedded in elastomeric substrate)									
193 graphene/MoS <sub>2</sub> /PDMS	H <sub>3</sub> PO <sub>4</sub> /PVA gel	30	0.88	300@30%	0.87	19.44 F cm <sup>-3</sup> @0.3 mA	0.8	Embedded within PDMS	Symmetric device
194 graphene/PDMS	PVP/NaCl gel	50	0.9	1000@50%	0.84	0.65 mF cm <sup>-2</sup> @50 mV s <sup>-1</sup>	1	Embedded within PDMS	Symmetric device
195 NCNT/PU	H <sub>3</sub> PO <sub>4</sub> /PVA gel	200	~1	1000@200%	0.98	37.6 mF cm <sup>-2</sup> @0.05 mA cm <sup>-2</sup>	1	Embedded within PU	Symmetric device
196 ACM/MWCNTs@PAA	ACM/ET <sub>4</sub> NBF <sub>4</sub> -ACN	50	~1	500@50%	~1	2.2 F cm <sup>-3</sup> @1 mA cm <sup>-2</sup>	2.7	Embedded within elastomer	Asymmetric device
197 GCP@PPY	Gold NPs/poly(acrylamide)	800	0.9	200@800%	0.72	835 mF cm <sup>-2</sup> @1 mA cm <sup>-2</sup>	1	Embedded within hydrogel	Symmetric device
198 Janus v-AuNWS	hydrogel	100	~1	1500@100%	0.91	60.8 $\mu$ F cm <sup>-2</sup> @20 mV s <sup>-1</sup>	0.8	Embedded within PDMS	Symmetric device
Flexible supercapacitors									
199 PANI/ZIF-67	H <sub>2</sub> SO <sub>4</sub> /PVA gel	n.a. <sup>c</sup>	n.a.	2000	0.8	35 mF cm <sup>-2</sup> @0.05 mA cm <sup>-2</sup>	1	Carbon cloth substrate	Symmetric device
150 2D porous carbon nanosheets	EMIMBF <sub>4</sub>	n.a.	n.a.	10 000	0.96	51.1 F cm <sup>-3</sup> @80 mA cm <sup>-3</sup>	4	Stainless steel mesh	Symmetric device
200 Ti <sub>3</sub> C <sub>2</sub> MXene	H <sub>2</sub> SO <sub>4</sub> /PVA gel	n.a.	n.a.	10 000	0.92	25 mF cm <sup>-2</sup> @20 mV s <sup>-1</sup>	0.6	Paper substrate	Symmetric device
201 v-AuNWS/PANI	H <sub>3</sub> PO <sub>4</sub> /PVA gel	n.a.	n.a.	5000	0.95	11.8 mF cm <sup>-2</sup> @10 mV s <sup>-1</sup>	0.8	PET substrate	Symmetric device

<sup>a</sup>  $C/C_0$  refers to the capacity retention of the battery either at the max strain or after the strain cycling. <sup>b</sup> n.r. = not reported. <sup>c</sup> n.a. = not applicable.

**5.2.1.2 Microstructure design.** This strategy involves a substrate that introduces a unique geometry through microstructural engineering design to impart stretchability, and these microstructured substrates are then coated with stiff active materials to enable strain. Chen and coworkers demonstrated a stretchable supercapacitor based on tripod-structured PDMS.<sup>175</sup> The tripod-structured PDMS was first stretched and transferred with GO microribbons and then released to form suspended GO wrinkles, as indicated in Fig. 10a. Conventional wrinkled structure endows stretchability that can accommodate the strain by changing its shape with an out-of-plane bend. However, the direct adhesive interfaces between the active materials and the elastomeric substrate are prone to cause large stress in the thin film of active materials, which severely restricts the electrochemical and mechanical stability of the device. The as-obtained wrinkle GO film was suspended on the stretchable substrate rather than direct-attached on it, and the gap between each tripod also provided free space to relieve tension, which significantly reduces the stress in the GO film and ensure the stability of supercapacitors under stretching/relaxing cycles (Fig. 10b). The resulting supercapacitors showed stable electrochemical performance under various strains (0–100%).

Another efficient way to fabricate structured substrates was proposed by Li *et al.*<sup>176</sup> A 3D-printing approach was introduced to fabricate patterned molds that produce concave wavy structured PDMS substrates (Fig. 10c). With sputtered gold as the current collector and the PANI/MWCNT composite slurry was injected into PDMS mold as the active material, the microsupercapacitors array achieved a high specific areal capacitance of 44.13 mF cm<sup>-2</sup> under 40% strain (Fig. 10d). Recently, another demonstration based on a structured substrate was reported by Lee *et al.*<sup>174</sup> A porous, deformable PDMS/Ecoflex substrate with micropores on the surface was fabricated by using sandpaper with roughness as a mold. The porous film is softer and more hydrophobic than the non-porous PDMS/Ecoflex film. Subsequently, patterned layers of a Cr/Au thin film, MWCNTs, and Mn/Mo mixed oxide were deposited *via* e-beam evaporation, spray coating, and electrodeposition, respectively (Fig. 10e). The normalized capacitance of as-obtained microsupercapacitors remained unchanged with increasing biaxial strain up to 50%. Furthermore, the capacitance retains ~90% of its initial value after 1000 stretching/relaxing cycles *via* application of steadily increasing strain from 10 to 50% (Fig. 10f).

**5.2.1.3 Folding (origami/kirigami) design.** The introduction of folding design into stretchable supercapacitors was first demonstrated by Nam *et al.*<sup>208</sup> An origami-based stretchable supercapacitor was demonstrated based on isolated graphite electrodes and a sectionalized gel electrolyte. Isolated graphite rods were first synthesized on cellular paper substrates and then a polymer gel electrolyte was deposited on the backsides so that the sectionalized gel electrolyte and isolated graphite electrodes were combined. The as-prepared origami-based supercapacitor could sustain a tensile strain of 30% without obvious electrochemical performance degradation. Another example

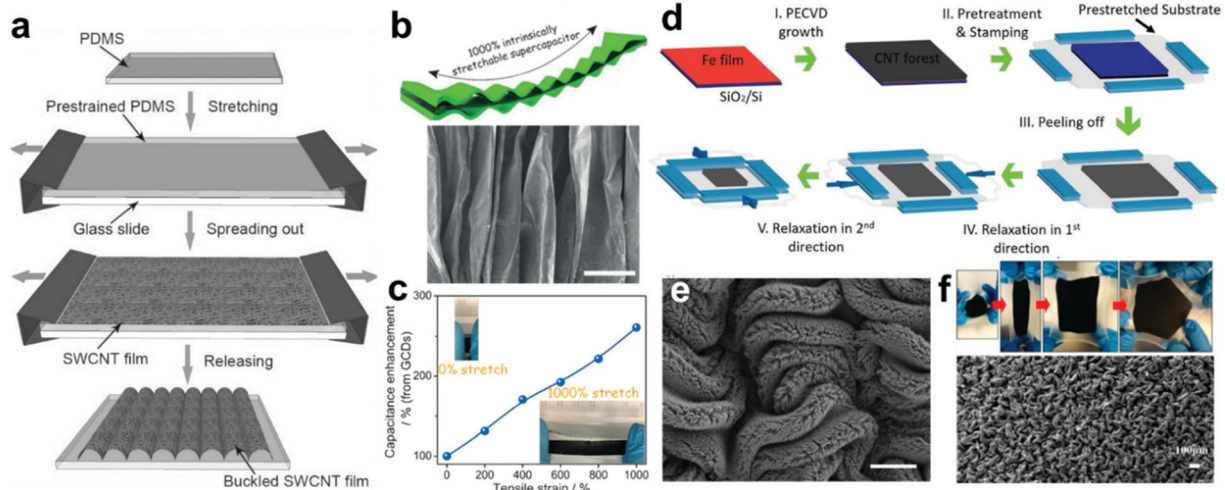


**Fig. 9** Fabrication of stretchable supercapacitors using the pre-strain method. (a) Schematic illustration of the preparation process for the buckled SWCNT film on PDMS.<sup>205</sup> Reprinted with permission from ref. 205. Copyright 2012 Wiley-VCH. (b) Schematic of the supercapacitor with accordion-like wavy structures. The resulting supercapacitors achieve ultra-high stretchability up to 1000%. (c) Capacitance enhancement under the increase of tensile strain.<sup>167</sup> Reprinted with permission from ref. 167. Copyright 2017 Wiley-VCH. (d) Schematic fabrication process flow of biaxially prestretched method. (e) SEM image of the crumpled structure on an elastomer substrate after relaxation in two directions.<sup>173</sup> Reprinted with permission from ref. 173. Copyright 2019 Wiley-VCH. (f) Omnidirectionally stretchable supercapacitor under various strain.<sup>170</sup> Reprinted with permission from ref. 170. Copyright 2016 American Chemical Society.

of a stretchable supercapacitor using a folding approach comes from Lv *et al.*<sup>178</sup> A 3D stretchable supercapacitor was made by attaching pieces of paper with adhesives into an internally expandable honeycomb lantern-like structure (Fig. 11a). The 3D structure with higher mass loading and enhanced specific areal capacitance are highly desired compared to 2D stretchable supercapacitors. The enhanced specific areal capacitance of such 3D supercapacitors ( $7.35 \text{ F cm}^{-2}$ ) is about 60 folds higher than that of its original 2D supercapacitor ( $120 \text{ mF cm}^{-2}$ ). The cycling stability test under repeated 2000% strain confirmed the excellent mechanical and electrochemical stability of the as-prepared supercapacitors. The capacitance remained very close to that of unstretched supercapacitors (97%) after 10 000 cycles (Fig. 11b). Moreover, this kind of supercapacitor can be shaped into customizable 3D shapes without losing their stretchability. As shown in Fig. 11c, five chair-shaped supercapacitors connected in series can be bent and stretched like an accordion.

In addition to the origami-based approach, there are distinguishing stretchable supercapacitors that also realized outstanding stretchability and even 3D stretchability through kirigami<sup>179,181,209,210</sup> or cutting-based editable techniques.<sup>180</sup> One well-known example of kirigami supercapacitors was reported by Chen and coworkers.<sup>180</sup> The kirigami-based editing process was conducted by cutting patterns on planar supercapacitors that could transform the supercapacitor sheet into customizable shapes, such as honeycomb-like structures, pyramid-like structures (Fig. 11d). Furthermore, the editing process can be operated after the connection of supercapacitors, achieving more complicated patterns while maintaining its electrochemical performance (Fig. 11e). Such 3D stretchable supercapacitors based on folding/cutting approaches show good electrochemical and mechanical performances, but unfortunately,

it may not be suitable for some skin-conformal applications of electronics where complicated and delicate paper-cutting is cost-prohibitive and intimate contact with skin is needed.

**5.2.2 Rigid islands stretchable supercapacitors.** Rigid islands layout with conductive interconnection designs have been widely studied to reduce the impact of applied tension strain on electrochemical performances for stretchable electronics.<sup>211</sup> Compared to conventional sandwich-type supercapacitors, microsupercapacitors require no separators and allow the reduction of the size and thickness of the whole device, allowing on-chip fabrication due to their planar configurations. In one demonstration, Ha *et al.* presented sputtered Ti/Au current collectors processed into serpentine interconnections between microsupercapacitors units, which imparts stretchability to microsupercapacitors array up to 30% strain (Fig. 12a and b).<sup>182</sup> However, a slight decrease of capacitance was observed upon stretching, which can be attributed to the deterioration of mechanical properties of conductors upon stretching, and thus only 30% strain capability of the final microsupercapacitors array was reported in this work. In an improvement of the rigid island method, Hong *et al.* reported a hybrid approach utilizing combined soft PDMS/Ecoflex substrates and stiff microsupercapacitors array patched with PET.<sup>184</sup> The strain applied to the entire system was accommodated by the soft part so that the impact on stiff microsupercapacitors was minimized. Finite element method analysis of strain distribution showed that under 40% uniaxial strain of the entire system, the rigid island where microsupercapacitors located only hold 7% strain while the soft part between islands can hold up to 120%.

In another advanced demonstration by Ha and coworkers, stiff PET films patched with microsupercapacitor units were embedded in the stretchable Ecoflex substrate, which formed a

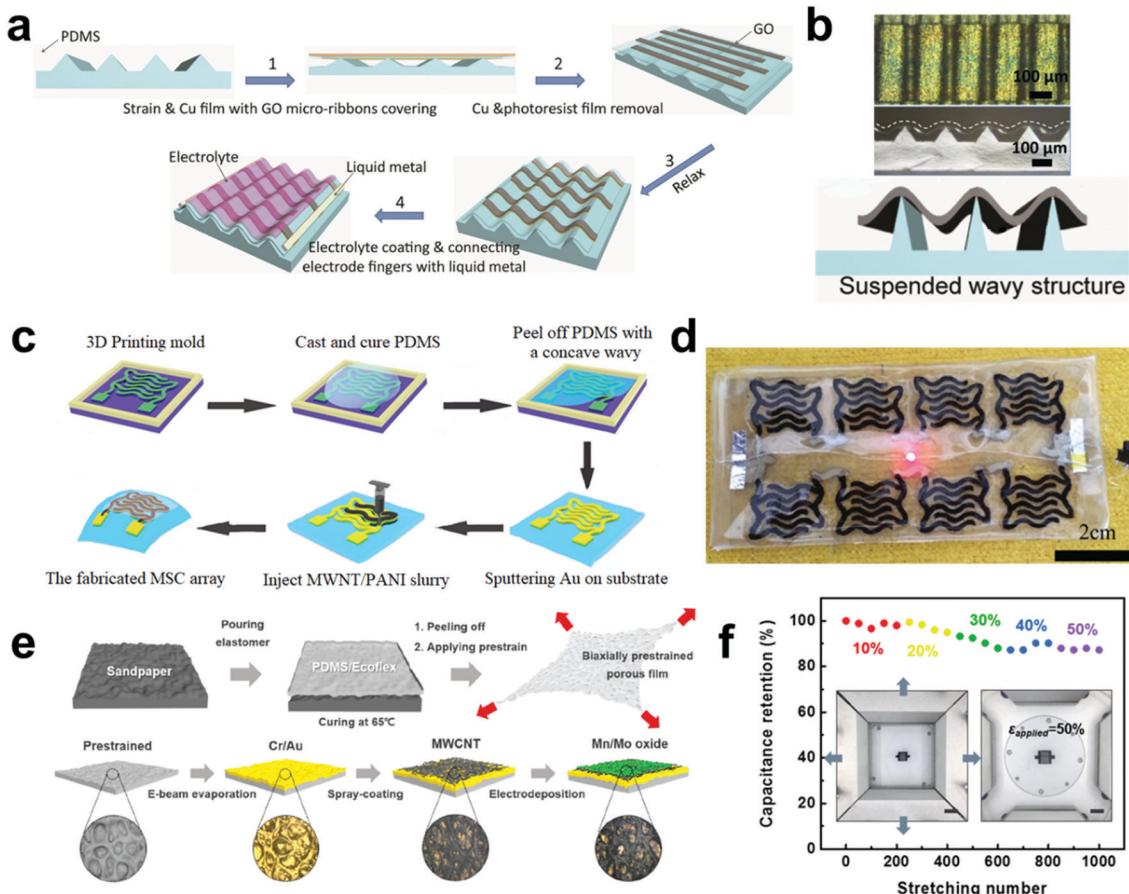


**Fig. 10** Fabrication of stretchable supercapacitors using microstructural design. (a) Transferring electrode arrays onto the tripod-structured PDMS substrate. (b) Optical images of the microsupercapacitors and its cross-sectional SEM image.<sup>175</sup> Reprinted with permission from ref. 175. Copyright 2015 Wiley-VCH. (c) Illustration to the fabrication of a stretchable MSC array with the concave wavy electrode. (d) Photograph of the concave wavy MSC array.<sup>176</sup> Reprinted with permission from ref. 176. Copyright 2017 Wiley-VCH. (e) Schematic illustration of the structure and fabrication process of a biaxially stretchable planar supercapacitor. (f) Capacitance retention as a function of stretching/relaxing cycle number under different biaxial strains.<sup>174</sup> Reprinted with permission from ref. 174. Copyright 2019 American Chemical Society.

strain suppressed zone so that the stiff microsupercapacitors can be exactly isolated from the strains (Fig. 12c).<sup>183</sup> The cross-section scheme of the stiff microsupercapacitor unit with ionogel electrolyte is shown in Fig. 12d. Besides, liquid metal and silver nanowires were used as the interconnection between microsupercapacitors array (Fig. 12e). The as-obtained system showed an extended stretchability of 100% under uniaxial strain and 50% under biaxial strain. Finite element method analysis confirms the microsupercapacitor array integrated on the stretchable Ecoflex substrate with implanted PET interlayer hardly deforms (Fig. 12f). The microsupercapacitor unit is almost undeformed as 0.02% and the stretchable substrate between two adjacent units is deformed up to 200%. Fig. 12g shows the CV curves of this system under various strains ranging from 0 to 50%. No observable change under a biaxial strain up to 50% was found. However, the system based on rigid microsupercapacitors array either connected by serpentine or embedded liquid metal interconnects usually provides low areal coverage. Ideal stretchable electrodes should have good areal coverage and excellent stretchability simultaneously.

**5.2.3 Fiber-shape stretchable supercapacitors.** From the perspective of device dimension, fiber or yarn-shaped supercapacitors have received tremendous attention in recent years as they can be woven into textiles and fabrics that breathe freely or can be integrated into different materials that fit the curved surface of the human body.<sup>212,213</sup> Thus, in this section, we aim to highlight selected strategies that can be used to make these fiber-like supercapacitors stretchable.

The first reported fiber-shape supercapacitors utilized CNT as active materials, and CNT sheets were wrapped around the elastic core rubber fiber and coated with the  $H_3PO_4/PVA$  gel electrolyte layer by layer to build a stretchable coaxial supercapacitor.<sup>186</sup> The resulting supercapacitor could be stretched to 75% tensile strain without sacrificing electrochemical performance ( $18 \text{ F g}^{-1}$ ) and maintain 90% capacity retention under 1000 stretching cycles. Another example to improve the specific capacitance is to use two CNT fibers deposited with  $MnO_2$  nanoparticles placed parallelly on a prestrained PDMS substrate and then covered with gel electrolyte (Fig. 13a).<sup>189</sup> The resulting supercapacitor delivered 40% stretchability and

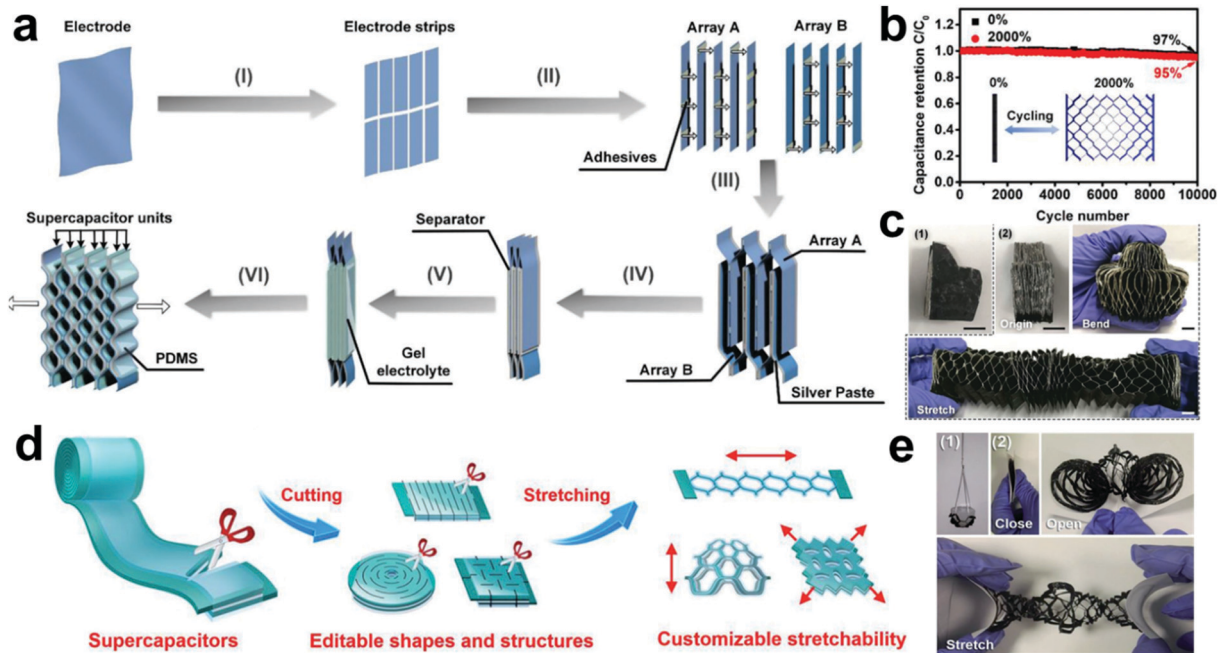


Fig. 11 Strategies to create foldable and stretchable supercapacitors. (a) Schematic drawing of the fabrication process for 3D stretchable supercapacitors. (b) Capacitance retention ratio of 3D stretchable supercapacitor based on PPy/BPO-CNT electrodes tested at  $7.8 \text{ mA cm}^{-2}$  under cycling tensile strain of 2000%. (c) 3D stretchable supercapacitors with chair shape under bending and stretching conditions.<sup>178</sup> Reprinted with permission from ref. 178. Copyright 2018 Wiley-VCH. (d) Schematics for the assembling process of stretchable supercapacitors through editable cutting strategy. (e) Editable supercapacitors with basket structures under different stretching states.<sup>180</sup> Reprinted with permission from ref. 180. Copyright 2017 Wiley-VCH.

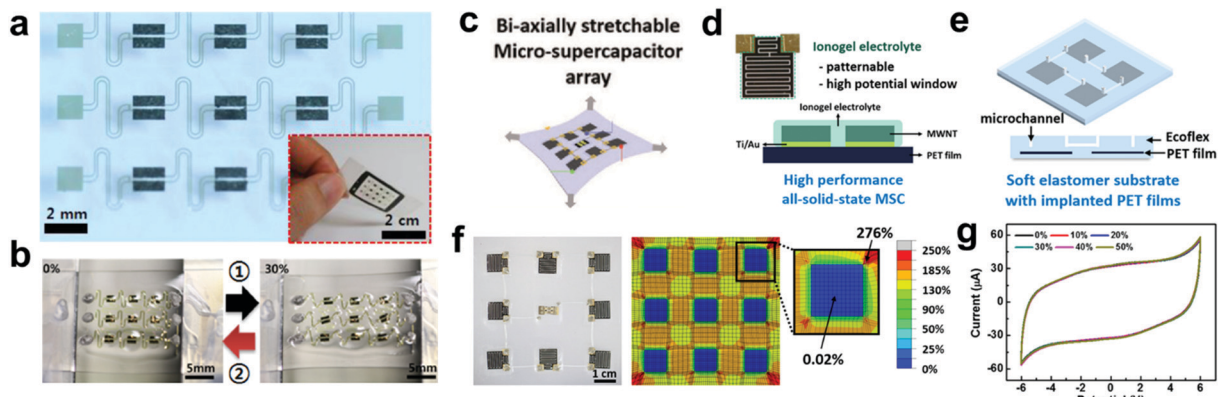
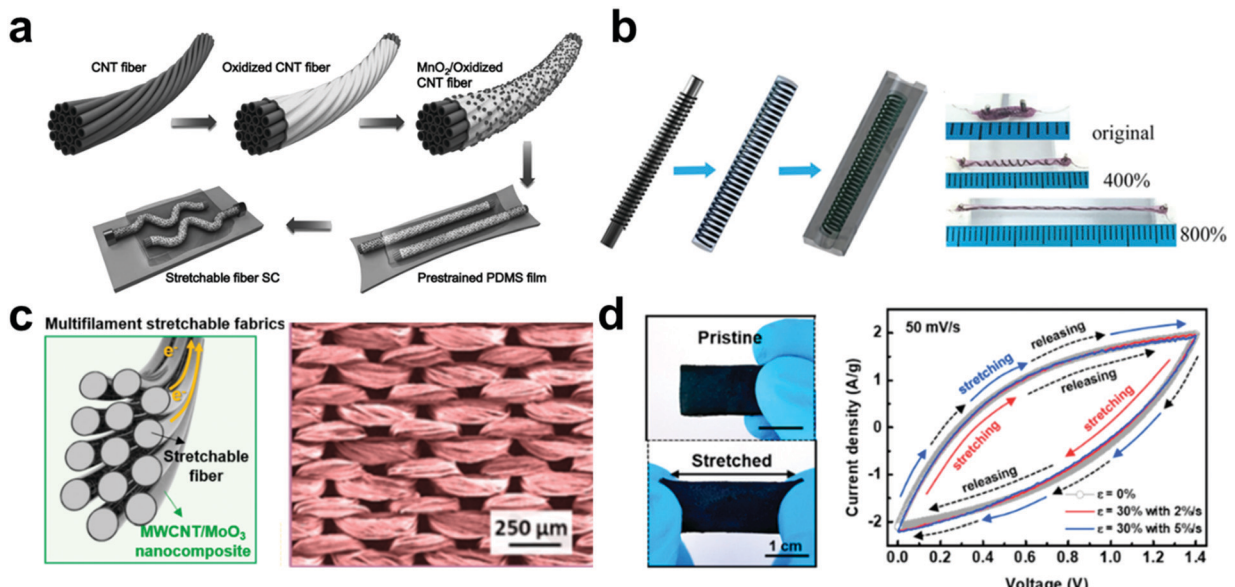


Fig. 12 Fabrication of stretchable supercapacitors using rigid island design. (a) Photograph of a stretchable MSC array on a PDMS substrate with the serpentine bridge. (b) Photographs of the entire device of MSC array before (left) and after application of strain of 30% (right).<sup>182</sup> Reprinted with permission from ref. 182. Copyright 2013 American Chemical Society. (c) Illustration of biaxially stretchable MSC array on a deformable substrate. (d) cross-section scheme of the MSC with ionogel electrolyte and embedded MSC. (e) Structure of the deformable substrate composed of Ecoflex with implanted PET films and embedded microchannel for liquid metal interconnection. (f) Optical image and FEM analysis of MSC array integrated on the stretchable substrate under 50% biaxial strains. (g) CV curves of MSC array upon biaxial stretching.<sup>183</sup> Reprinted with permission from ref. 183. Copyright 2014 American Chemical Society.

provide a high specific volumetric capacitance of around  $409.4 \text{ F cm}^{-3}$ .

The fiber-like electrodes can be further enwound at the external side of a glass rod and remolded into a spring-like structure. Yu and co-workers demonstrated a self-standing fiber electrode fabricated *via* macromolecular self-assembly of GO and PANI hydrogels, exhibiting an excellent flexibility compared with most studied fiber-shaped supercapacitors and

therefore can be remolded into spring-like shapes.<sup>214</sup> Another spring-like design was proposed by Lu *et al.* to develop a superelastic fiber-based supercapacitor.<sup>190</sup> Briefly, the hybrid graphene/CNT/PANI wires were synthesized and twisted to form non-stretchable fiber supercapacitors. Then, the as-prepared fiber was coiled on a rod into a spring-like configuration, followed by casting with a thin layer of SEBS polymer to fix the spring structure (Fig. 13b). The electrochemical performance



**Fig. 13** Stretchable supercapacitors using fiber shape design. (a) Schematic illustration of the fabrication process of the fiber supercapacitor with parallel topology.<sup>189</sup> Reprinted with permission from ref. 189. Copyright 2017 Wiley-VCH. (b) Schematic illustration of the fabrication of a spring-like supercapacitor (left). Photograph of as-prepared supercapacitor with different strains up to 800% (right).<sup>190</sup> Reprinted with permission from ref. 190. Copyright 2017 Wiley-VCH. (c) Cross-sectional illustration (left) and SEM images (right) of the stretchable fiber showing the multifilament structure and MWCNT/MoO<sub>3</sub> nanocomposite in the fabric. (d) Optical images and CV curves measured during dynamic stretching/releasing cycles at 30% strain with different strain rates.<sup>192</sup> Reprinted with permission from ref. 192. Copyright 2019 American Chemical Society.

was well-preserved under a maximum strain of 800% with a specific capacitance of 138 F g<sup>-1</sup>.

Another popular strategy to fabricate stretchable supercapacitors is to use the textile technology.<sup>215–217</sup> Textiles with knitted structures can be intrinsically stretched because the meandering loops can be extended in different directions. Park *et al.* demonstrated a textile-based supercapacitor integrated with a textile-based strain sensor.<sup>192</sup> The hybrid composite of MoO<sub>3</sub> nanowires/MWCNT was synthesized and spray-coated on the stretchable fabric substrate (nylon (82%)/Spandex (18%)). The capacitance retention is 80% after 5000 stretching/relaxing cycles of increasing strain from 10 to 50%. And the electrochemical performance remained nearly unchanged under 30% dynamic stretching at various strain rates (Fig. 13d). Although this report demonstrated successful integration of textile-based supercapacitors and strain sensors, still, energy harvesting for wireless charging of the supercapacitor needs to be studied and added into the integrated system for more practical applications.

There are several challenges remained for practical integrations of fiber-like energy storage devices and other functional devices: (1) to fabricate high-performance fiber-shaped devices at low cost. The process for fabricating multiple coaxial layers onto a core fiber substrate is technically complex. Also, packaging process requires extra cost and increase the total dimension and weight of fiber-shape devices (2) the operation environments for wearable electronics often require devices withstanding repeated squeezing or bending deformations caused by body movements. Under these circumstances, such deformation will inevitably lead to significant performance

degradation over long term. (3) Washability is another critical issue when integrating various fiber devices into a textile or garment. Therefore, developing novel packaging materials with long term durability is also a primary problem that needs to be solved as soon as possible.

**5.2.4 Toward intrinsically stretchable supercapacitors.** We have reviewed the recent progress of flexible supercapacitors as well as included the approaches for the creation of stretchable supercapacitors. However, the current fabrication strategies mentioned previously mainly adopted geometric engineering, which is costly and complicated, and some of the as-fabricated devices still hold unsatisfactory strain. Furthermore, the polymer gel electrolyte sandwiched between the two electrodes results in a dense packing of active materials, leading to unsatisfactory electrochemical performance and limited stretchability (<100% in most cases) due to delamination issue. The key to fabricating high-performance stretchable supercapacitors is the design of intrinsic stretchability for each component of supercapacitors. It is urgent and challenging to design an integrated and intrinsically stretchable device, which can prevent the misalignment/delamination of the devices during repeated stretching/releasing cycles.

Recently, some researchers have been dedicated to the development of integrated and intrinsically stretchable supercapacitors. Chen *et al.* reported a strategy to prepare a stretchable polypyrrole-incorporated gold nanoparticle/CNT/poly(acrylamide) (GCP@PPy) hydrogel supercapacitor, which can be linearly stretched by 800% with excellent capacitance retention upon stretching.<sup>197</sup> The device was assembled by sandwiching GCP@PPy electrodes with a GP hydrogel electrolyte with the

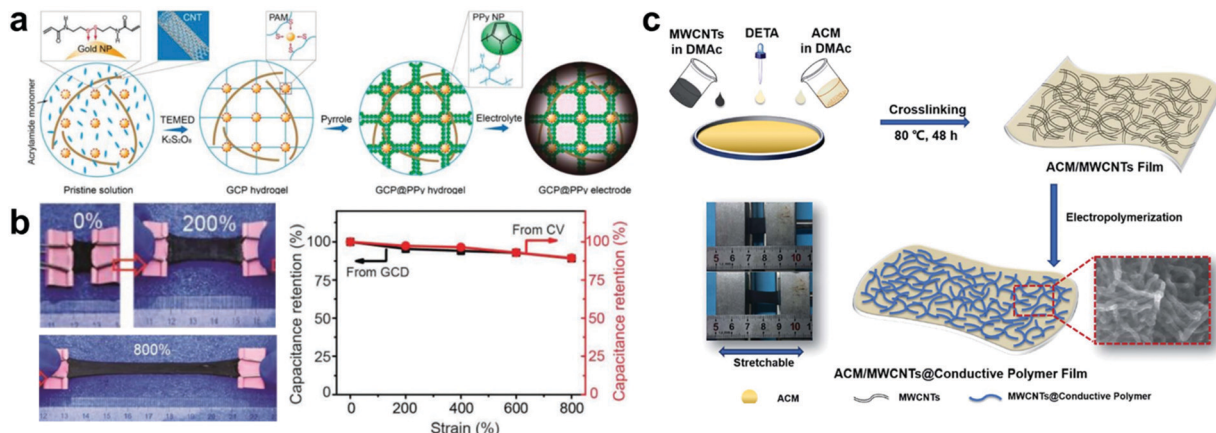


Fig. 14 Toward Intrinsically stretchable supercapacitors. (a) Schematic illustration of the preparation of the GCP@PPy electrode. (b) Optical images showing high stretchability of the device (left) and capacitance retention under various strains.<sup>197</sup> Reprinted with permission from ref. 197. Copyright 2019 Wiley-VCH. (c) Schematic diagram of the fabrication of stretchable ACM/MWCNTs@conductive polymer film electrodes.<sup>196</sup> Reproduced with permission from ref. 196. Copyright 2018 Royal Society of Chemistry.

integrated electrode–electrolyte–electrode structure arising from reconstruction of Au–thiolate (Au–SR) bonds under NIR laser irradiation. AgNW film layer was sprayed onto the electrode surface to act as the current collector, and it was tightly soldered onto the electrode layer and demonstrated stretchability and healability.

Another example of integrally and intrinsically stretchable supercapacitors was demonstrated by Wang *et al.*<sup>196</sup> In this work, acrylate rubber/multiwall carbon nanotube (ACM/MWCNT) composite film was used to create intrinsically stretchable electrolyte (Fig. 14c).<sup>59</sup> Because of the characteristic of absorbing organic solution of the ACM matrix, the monomers can easily penetrate ACM/MWCNT films for electrodepositing conductive polymers (poly(1,5-diaminoanthraquinone) (PDA), and polyaniline (PANI)) ACM/MWCNT supported conductive polymers (ACM/MWCNT@PANI; ACM/MWCNT@PDA) were used as cathode and anode. The stretchable electrodes and the electrolyte use the same kind of ACM matrix material, which can improve the affinity and contact between them. The electrochemical performance of the as-assembled supercapacitor remains unchanged under 50% strain for 300 stretching cycles.

Overall, there are many strategies that have been pursued to develop stretchable supercapacitor devices. Each strategy has its own unique advantages, and could be used depending on the application in mind. As always, balancing the performance of the resulting device with the simplicity of design is a challenge. Fortunately, the wide range of materials used for supercapacitors allows for a large design space for creating stretchable devices. In the end, it is likely that a combination of strategies is needed to make a high performance, strain-compliant, long-lasting and well-integrated design for energy storage for wearable electronics.

## 6. Conclusion and future outlook

The development of soft, stretchable, and conformal energy storage systems will be crucial to enable skin-compatible

wearable electronics. While the development of wearable electronic devices currently outpaces the development of stretchable power sources, much progress has been made in the last 10 years. In this review, we highlighted that while flexible energy sources have received more attention than stretchable batteries and supercapacitors, the performance of stretchable devices is beginning to catch up. With sufficient development, these deformable battery technologies would improve wearable technologies that already exist on the market. Good examples of commercial wearable devices that could benefit from a conformable battery include on-skin bio-metric patches (MC10, *etc.*) as well as on-skin iontophoretic patches (Iontopatch).

Further development of stretchable electrochemical energy storage systems requires careful consideration of several factors. We have highlighted several strategies that can be used to create stretchable devices. Namely, these strategies are; wavy structure, microstructure, folding, rigid-islands, fiber-like, and intrinsically stretchable. While no specific strategy is the best for every material or application, each strategy may have individual benefits. For example, wavy structures and rigid-island structures generally have only minor changes in electrochemical performance when subjected to strain. Rigid-island stretchability has the advantage of being able to utilize conventional active materials, enabling a wide range of materials selection and modification. Microstructuring strategies generally enable isotropic strain capability, and also open up modularity for tuning the mechanical properties of the individual components. Intrinsically stretchable batteries have the advantage of being easy to fabricate and may ultimately be able to achieve the highest energy density, if the amount of inactive materials can be kept to a minimum.

Regardless of which strategy is pursued, there are some common themes and future studies that should be acknowledged when developing stretchable energy storage systems for wearable electronics.

(1) Strain capability and conformability: so far, while each strategy has shown the ability to enable stretchability, typically

the strategies involving rigid-island, fiber-like, or folding structures have shown the largest deformation capability. However, these devices often are not omnidirectionally stretchable, which may limit their applicability. Devices based on intrinsically stretchable components are typically isotopically stretchable, but currently have lower strain capability. When designing stretchable devices, the required strain capability of the final application should also be considered.

(2) Energy density: achieving high energy density while maintaining stretchability is a challenge. Often, the ability to handle more strain comes at the expense of energy density. In this way, microstructured or intrinsically stretchable devices stand out as a potential method to have good energy density and stretchability, as these strategies do not require substantial amounts of inactive materials.

(3) Safety: regardless of the mechanism of stretchability/energy storage used, the safety of the electrochemical energy storage device is crucial for wearable electronics applications. So far, promising strategies include using robust electrolyte materials such as crosslinked polymers as well as using aqueous electrolytes. Future works in the field of stretchable energy storage should also consider factors such as cut-and-puncture testing as well as device flammability.

(4) Cost: little work has been done to analyze the projected costs of these stretchable energy storage systems, which will have a dramatic impact on their potential commercialization. Of the different device chemistries and stretchability strategies discussed in this review, the costs may vary widely. In general, it is beneficial to use existing manufacturing processes and to try to introduce as few additional steps as possible when fabricating stretchable electronics. The exploration of unique and scalable fabrication protocols is also encouraged in order to reduce costs. Techniques such as screen printing, inkjet printing,<sup>218,219</sup> and additive manufacturing<sup>220</sup> are interesting for creating cost-effective stretchable energy storage devices.

(5) Durability: so far, researchers have demonstrated stability of devices over tens of thousands of cycles, as well as washability in some cases. However, in many devices, problems such as delamination or degradation may cause reductions in performance. Durability in cycle life due to packaging is also a major consideration. Researchers need to spend more time identifying stretchable, hermetic packaging materials that allow for long-term battery operation even under deformation and variable environmental conditions.

(6) Integration: the combination of these stretchable energy sources with actual wearable electronics should be demonstrated. Some applications of wearable electronics will require features such as thinness, softness, and skin-conformability.<sup>221</sup> It is also likely that some form of control circuitry is required to handle the minor variations in power output during deformation, and a more in-depth understanding of how these devices integrate with commercial wearables would be informative.

Overall, the future of stretchable power sources is bright. By combining several of the strategies covered in this review, we believe that it will be possible to identify the right materials

to enable high-performance and practical deformable power sources.

## Conflicts of interest

The authors declare no conflicts of interest.

## Acknowledgements

Y. C. and Z. B. acknowledge the support by Samsung Electronics. The authors acknowledge the support from the Assistant Secretary for Energy Efficiency and Renewable Energy, Office of Vehicle Technologies of the U.S. Department of Energy through the Advanced Battery Materials Research (BMR) Program and Battery500 Consortium. D. G. M. acknowledges support by the National Science Foundation Graduate Research Fellowship Program under Grant No. (DGE-114747).

## References

- 1 W. Song, S. Yoo, G. Song, S. Lee, M. Kong, J. Rim, U. Jeong and S. Park, *Batter. Supercaps*, 2019, **2**, 181–199.
- 2 A. M. Zamarayeva, A. E. Ostfeld, M. Wang, J. K. Duey, I. Deckman, B. P. Lechêne, G. Davies, D. A. Steingart and A. C. Arias, *Sci. Adv.*, 2017, **3**, e1602051.
- 3 J. Xu, S. Wang, G. J. N. Wang, C. Zhu, S. Luo, L. Jin, X. Gu, S. Chen, V. R. Feig, J. W. F. To, S. Rondeau-Gagné, J. Park, B. C. Schroeder, C. Lu, J. Y. Oh, Y. Wang, Y. H. Kim, H. Yan, R. Sinclair, D. Zhou, G. Xue, B. Murmann, C. Linder, W. Cai, J. B. H. Tok, J. W. Chung and Z. Bao, *Science*, 2017, **355**, 59–64.
- 4 S. Wang, J. Xu, W. Wang, G. J. N. Wang, R. Rastak, F. Molina-Lopez, J. W. Chung, S. Niu, V. R. Feig, J. Lopez, T. Lei, S. K. Kwon, Y. Kim, A. M. Foudeh, A. Ehrlich, A. Gasperini, Y. Yun, B. Murmann, J. B. H. Tok and Z. Bao, *Nature*, 2018, **555**, 83–88.
- 5 D. Son, J. Kang, O. Vardoulis, Y. Kim, N. Matsuhisa, J. Y. Oh, J. W. F. To, J. Mun, T. Katsumata, Y. Liu, A. F. McGuire, M. Krason, F. Molina-lopez, J. Ham, U. Kraft, Y. Lee, Y. Yun, J. B. Tok and Z. Bao, *Nat. Nanotechnol.*, 2018, **13**, 1057–1066.
- 6 C. M. Boutil, Y. Kaizawa, B. C. Schroeder, A. Chortos, A. Legrand, Z. Wang, J. Chang, P. Fox and Z. Bao, *Nat. Electron.*, 2018, **1**, 314–321.
- 7 B. Chu, W. Burnett, J. W. Chung and Z. Bao, *Nature*, 2017, **549**, 328–330.
- 8 S. Niu, N. Matsuhisa, L. Beker, J. Li, S. Wang, J. Wang, Y. Jiang, X. Yan, Y. Yun, W. Burnett, A. S. Y. Poon, J. B. H. Tok, X. Chen and Z. Bao, *Nat. Electron.*, 2019, **2**, 361–368.
- 9 J. Liu, T. M. Fu, Z. Cheng, G. Hong, T. Zhou, L. Jin, M. Duvvuri, Z. Jiang, P. Kruskal, C. Xie, Z. Suo, Y. Fang and C. M. Lieber, *Nat. Nanotechnol.*, 2015, **10**, 629–635.
- 10 Y. Liu, J. Liu, S. Chen, T. Lei, Y. Kim, S. Niu, H. Wang, X. Wang, A. M. Foudeh, J. B. H. Tok and Z. Bao, *Nat. Biomed. Eng.*, 2019, **3**, 58–68.

11 P. G. Agache, C. Monneur, J. L. Leveque and J. De Rigal, *Arch. Dermatol. Res.*, 1980, **269**, 221–232.

12 A. Chortos and Z. Bao, *Mater. Today*, 2014, **17**, 321–331.

13 J. C. Yang, J. Mun, S. Y. Kwon, S. Park, Z. Bao and S. Park, *Adv. Mater.*, 2019, **31**, 1904765, DOI: 10.1002/adma.201904765.

14 P. V. Braun and R. G. Nuzzo, *Nat. Nanotechnol.*, 2014, **9**, 962–963.

15 A. Sumboja, J. Liu, W. G. Zheng, Y. Zong, H. Zhang and Z. Liu, *Chem. Soc. Rev.*, 2018, **47**, 5919–5945.

16 B. Sun, Y.-Z. Long, Z.-J. Chen, S.-L. Liu, H.-D. Zhang, J.-C. Zhang and W.-P. Han, *J. Mater. Chem. C*, 2014, **2**, 1209–1219.

17 C. J. Bettinger, *Bioelectron. Med.*, 2018, **4**, 6.

18 Y. Liu, Y. Zhu and Y. Cui, *Nat. Energy*, 2019, **4**, 540–550.

19 Z. J. Zhang and P. Ramadass, *Lithium-Ion Batteries*, Springer New York, New York, NY, 2009, pp. 1–46.

20 T. Nishida, *Lithium-Ion Batteries*, Springer New York, New York, NY, 2009, pp. 1–13.

21 C. Bommier and X. Ji, *Small*, 2018, **14**, 1–20.

22 G. Wang, L. Zhang and J. Zhang, *Chem. Soc. Rev.*, 2012, **41**, 797–828.

23 B. E. Conway, V. Birss and J. Wojtowicz, *J. Power Sources*, 1997, **66**, 1–14.

24 G. Wang, L. Zhang and J. Zhang, *Chem. Soc. Rev.*, 2012, **41**, 797–828.

25 A. González, E. Goikolea, J. A. Barrena and R. Mysyk, *Renewable Sustainable Energy Rev.*, 2016, **58**, 1189–1206.

26 G. Wang, L. Zhang and J. Zhang, *Chem. Soc. Rev.*, 2012, **41**, 797–828.

27 D. G. Mackanic, X. Yan, Q. Zhang, N. Matsuhsisa, Z. Yu, Y. Jiang, T. Manika, J. Lopez, H. Yan, K. Liu, X. Chen, Y. Cui and Z. Bao, *Nat. Commun.*, 2019, **10**, 5384.

28 Y. Xie, Y. Liu, Y. Zhao, Y. H. Tsang, S. P. Lau, H. Huang and Y. Chai, *J. Mater. Chem. A*, 2014, **2**, 9142–9149.

29 T. Ma, G. L. Xu, Y. Li, L. Wang, X. He, J. Zheng, J. Liu, M. H. Engelhard, P. Zapol, L. A. Curtiss, J. Jorne, K. Amine and Z. Chen, *J. Phys. Chem. Lett.*, 2017, **8**, 1072–1077.

30 W. Liu, N. Liu, J. Sun, P. C. Hsu, Y. Li, H. W. Lee and Y. Cui, *Nano Lett.*, 2015, **15**, 2740–2745.

31 J. F. Snyder, M. A. Ratner and D. F. Shriver, *Solid State Ionics*, 2002, **147**, 249–257.

32 W. Liu, S. W. Lee, D. Lin, F. Shi, S. Wang, A. D. Sendek and Y. Cui, *Nat. Energy*, 2017, **2**, 17035.

33 J. Bae, Y. Li, J. Zhang, X. Zhou, F. Zhao, Y. Shi, J. B. Goodenough and G. Yu, *Angew. Chem., Int. Ed.*, 2018, **57**, 2096–2100.

34 Y. Liu, D. Lin, Y. Jin, K. Liu, X. Tao, Q. Zhang, X. Zhang and Y. Cui, *Sci. Adv.*, 2017, **3**(10), eaao0713.

35 L. Yue, J. Ma, J. Zhang, J. Zhao, S. Dong, Z. Liu, G. Cui and L. Chen, *Energy Storage Mater.*, 2016, **5**, 139–164.

36 D. G. Mackanic, W. Michaels, M. Lee, D. Feng, J. Lopez, J. Qin, Y. Cui and Z. Bao, *Adv. Energy Mater.*, 2018, **8**, 1800703.

37 M. Park, X. Zhang, M. Chung, G. B. Less and A. M. Sastry, *J. Power Sources*, 2010, **195**, 7904–7929.

38 S. Zhang, N. Nguyen, B. Leonhardt, C. Jolowsky, A. Hao, J. G. Park and R. Liang, *Adv. Electron. Mater.*, 2019, **5**, 1–36.

39 N. Matsuhsisa, X. Chen, Z. Bao and T. Someya, *Chem. Soc. Rev.*, 2019, **48**, 2946–2966.

40 P. P.-J. Chu, M. Tsai and Y. S. Hsieh, *Meet. Abstr.*, 2017, **MA2017-01**, 28.

41 W. Liu, Z. Chen, G. Zhou, Y. Sun, H. R. Lee, C. Liu, H. Yao, Z. Bao and Y. Cui, *Adv. Mater.*, 2016, **28**, 3578–3583.

42 P. Y. Chen, M. Zhang, M. Liu, I. Y. Wong and R. H. Hurt, *ACS Nano*, 2018, **12**, 234–244.

43 S. Kang, S. Y. Hong, N. Kim, J. Oh, M. Park, K. Y. Chung, S.-S. Lee, J. Lee and J. G. Son, *ACS Nano*, 2020, **14**, 3660–3668.

44 H. Kim, Y. Miura and C. W. MacOsko, *Chem. Mater.*, 2010, **22**, 3441–3450.

45 P. Le Floch, S. Meixuanzi, J. Tang, J. Liu and Z. Suo, *ACS Appl. Mater. Interfaces*, 2018, **10**, 27333–27343.

46 G. Kettlgruber, M. Kaltenbrunner, C. M. Siket, R. Moser, I. M. Graz, R. Schwödiauer and S. Bauer, *J. Mater. Chem. A*, 2013, **1**, 5505–5508.

47 J. Liu, M. Hu, J. Wang, N. Nie, Y. Wang, Y. Wang, J. Zhang and Y. Huang, *Nano Energy*, 2019, **58**, 338–346.

48 E.-H. Ko, H.-J. Kim, S.-M. Lee, T.-W. Kim and H.-K. Kim, *Sci. Rep.*, 2017, **7**, 46739.

49 H. Lee, J. K. Yoo, J. H. Park, J. H. Kim, K. Kang and Y. S. Jung, *Adv. Energy Mater.*, 2012, **2**, 976–982.

50 K. Fukue, Y. Iwata and E. Iwase, Design of Substrate Stretchability Using Origami-Like Folding Deformation for Flexible Thermoelectric Generator, *Micromachines*, 2018, **9**(7), 315, DOI: 10.3390/mi9070315.

51 Z. Song, X. Wang, C. Lv, Y. An, M. Liang, T. Ma, D. He, Y. J. Zheng, S. Q. Huang, H. Yu and H. Jiang, *Sci. Rep.*, 2015, **5**, 1–9.

52 S. Isah, *Asian J. Nanosci. Mater.*, 2018, **1**, 90–103.

53 S. Pan, J. Ren, X. Fang and H. Peng, *Adv. Energy Mater.*, 2016, **6**, 1501867.

54 A. M. V. Mohan, N. Kim, Y. Gu, A. J. Bandodkar, J.-M. You, R. Kumar, J. F. Kurniawan, S. Xu and J. Wang, *Adv. Mater. Technol.*, 2017, **2**, 1600284.

55 D. J. Lipomi and Z. Bao, *Energy Environ. Sci.*, 2011, **4**, 3314–3328.

56 M. Liao, L. Ye, Y. Zhang, T. Chen and H. Peng, *Adv. Electron. Mater.*, 2019, **5**, 1–14.

57 D. Ren, L. Dong, J. Wang, X. Ma, C. Xu and F. Kang, *ChemistrySelect*, 2018, **3**, 4179–4184.

58 Z. Wang, J. Cheng, Q. Guan, H. Huang, Y. Li, J. Zhou, W. Ni, B. Wang, S. He and H. Peng, *Nano Energy*, 2018, **45**, 210–219.

59 J. Yu, J. Zhou, P. Yao, J. Huang, W. Sun, C. Zhu and J. Xu, *J. Power Sources*, 2019, **440**, 227150.

60 T. An and W. Cheng, *J. Mater. Chem. A*, 2018, **6**, 15478–15494.

61 Y. Zheng, G. J. N. Wang, J. Kang, M. Nikolka, H. C. Wu, H. Tran, S. Zhang, H. Yan, H. Chen, P. Y. Yuen, J. Mun, R. H. Dauskardt, I. McCulloch, J. B. H. Tok, X. Gu and Z. Bao, *Adv. Funct. Mater.*, 2019, **29**, 1–12.

62 G. J. N. Wang, A. Gasperini and Z. Bao, *Adv. Electron. Mater.*, 2018, **4**, 1–21.

63 P. Simon, Y. Gogotsi and B. Dunn, *Science*, 2014, **343**, 1210–1211.

64 Y. Liu, M. Pharr and G. A. Salvatore, *ACS Nano*, 2017, **11**, 9614–9635.

65 W. Liu, M.-S. Song, B. Kong and Y. Cui, Flexible and Stretchable Energy Storage: Recent Advances and Future Perspectives, *Adv. Mater.*, 2016, **29**, 1603436, DOI: 10.1002/adma.201603436.

66 D. J. Lipomi and Z. Bao, *MRS Bull.*, 2017, **42**, 93–97.

67 L. Wang, D. Chen, K. Jiang and G. Shen, *Chem. Soc. Rev.*, 2017, **46**, 6764–6815.

68 S. Bauer, *Nat. Mater.*, 2013, **12**, 871–872.

69 H. J. Peng, J. Q. Huang and Q. Zhang, *Chem. Soc. Rev.*, 2017, **46**, 5237–5288.

70 G. Zhou, F. Li and H. M. Cheng, *Energy Environ. Sci.*, 2014, **7**, 1307–1338.

71 M. Yousaf, H. T. H. Shi, Y. Wang, Y. Chen, Z. Ma, A. Cao, H. E. Naguib and R. P. S. Han, *Adv. Energy Mater.*, 2016, **6**, 1600490.

72 Y. Khan, A. Thielens, S. Muin, J. Ting, C. Baumbauer and A. C. Arias, *Adv. Mater.*, 2019, **1905279**, 1905279.

73 A. M. Gaikwad, B. V. Khau, G. Davies, B. Hertzberg, D. A. Steingart and A. C. Arias, *Adv. Energy Mater.*, 2015, **5**, 1–11.

74 Y. H. Lee, J. S. Kim, J. Noh, I. Lee, H. J. Kim, S. Choi, J. Seo, S. Jeon, T. S. Kim, J. Y. Lee and J. W. Choi, *Nano Lett.*, 2013, **13**, 5753–5761.

75 S. Cao, X. Feng, Y. Song, H. Liu, M. Miao, J. Fang and L. Shi, *ACS Appl. Mater. Interfaces*, 2016, **8**, 1073–1079.

76 S. Yoon, S. Lee, S. Kim, K. W. Park, D. Cho and Y. Jeong, *J. Power Sources*, 2015, **279**, 495–501.

77 A. Abnavi, M. Sadati Faramarzi, A. Abdollahi, R. Ramzani, S. Ghasemi and Z. Sanaee, *Nanotechnology*, 2017, **28**, 255404.

78 T. H. Nguyen, A. Fraiwan and S. Choi, *Biosens. Bioelectron.*, 2014, **54**, 640–649.

79 M. Mohammadifar and S. Choi, On-Demand Micro-Power Generation from an Origami-Inspired Paper Biobattery Stack, *Batteries*, 2018, **4**(2), 14, DOI: 10.3390/batteries 4020014.

80 S. H. Kim, K. H. Choi, S. J. Cho, S. Choi, S. Park and S. Y. Lee, *Nano Lett.*, 2015, **15**, 5168–5177.

81 N. Singh, C. Galande, A. Miranda, A. Mathkar, W. Gao, A. L. M. Reddy, A. Vlad and P. M. Ajayan, *Sci. Rep.*, 2012, **2**, 6–10.

82 S. Berchmans, A. J. Bandodkar, W. Jia, J. Ramírez, Y. S. Meng and J. Wang, *J. Mater. Chem. A*, 2014, **2**, 15788–15795.

83 M. Koo, K. Il Park, S. H. Lee, M. Suh, D. Y. Jeon, J. W. Choi, K. Kang and K. J. Lee, *Nano Lett.*, 2012, **12**, 4810–4816.

84 J. Janek and W. G. Zeier, *Nat. Energy*, 2016, **1**, 16141.

85 C. Yang, X. Ji, X. Fan, T. Gao, L. Suo, F. Wang, W. Sun, J. Chen, L. Chen, F. Han, L. Miao, K. Xu, K. Gerasopoulos and C. Wang, *Adv. Mater.*, 2017, **29**, 1–8.

86 A. M. Gaikwad, A. C. Arias and D. A. Steingart, *Energy Technol.*, 2014, **3**, 305–328.

87 J. D. MacKenzie and C. Ho, *Proc. IEEE*, 2015, **103**, 535–553.

88 M. J. Lain, J. Brandon and E. Kendrick, Design Strategies for High Power vs. High Energy Lithium Ion Cells, *Batteries*, 2019, **5**, 64.

89 W. J. Song, S. Lee, G. Song and S. Park, *ACS Energy Lett.*, 2019, **4**, 177–186.

90 S. Kwak, J. Kang, I. Nam and J. Yi, *Micromachines*, 2020, **11**, 347.

91 H. Li, X. Zhang, Z. Zhao, Z. Hu, X. Liu and G. Yu, *Energy Storage Mater.*, 2020, **26**, 83–104.

92 W. Weng, Q. Sun, Y. Zhang, S. He, Q. Wu, J. Deng, X. Fang, G. Guan, J. Ren and H. Peng, *Adv. Mater.*, 2015, **27**, 1363–1369.

93 W. Liu, J. Chen, Z. Chen, K. Liu, G. Zhou, Y. Sun, M. S. Song, Z. Bao and Y. Cui, *Adv. Energy Mater.*, 2017, **7**, 1–6.

94 A. M. Gaikwad, A. M. Zamarayeva, J. Rousseau, H. Chu, I. Derin and D. A. Steingart, *Adv. Mater.*, 2012, **24**, 5071–5076.

95 M. Shin, W. Song, H. Bin Son, S. Yoo, S. Kim, G. Song, N. Choi and S. Park, *Adv. Energy Mater.*, 2018, **1801025**, 1–10.

96 W. J. Song, J. Park, D. H. Kim, S. Bae, M. J. Kwak, M. Shin, S. Kim, S. Choi, J. H. Jang, T. J. Shin, S. Y. Kim, K. Seo and S. Park, *Adv. Energy Mater.*, 2018, **8**, 1–10.

97 Y. Sun, J. Lopez, H.-W. Lee, N. Liu, G. Zheng, C.-L. Wu, J. Sun, W. Liu, J. W. Chung, Z. Bao and Y. Cui, *Adv. Mater.*, 2016, **28**, 2455–2461.

98 W. Liu, Z. Chen, G. Zhou, Y. Sun, H. R. Lee, C. Liu, H. Yao, Z. Bao and Y. Cui, *Adv. Mater.*, 2016, **28**, 3578–3583.

99 H. Li, Y. Ding, H. Ha, Y. Shi, L. Peng, X. Zhang, C. J. Ellison and G. Yu, *Adv. Mater.*, 2017, **29**, 1700898.

100 H. W. Zhu, J. Ge, Y. C. Peng, H. Y. Zhao, L. A. Shi and S. H. Yu, *Nano Res.*, 2018, **11**, 1554–1562.

101 C. Yan, X. Wang, M. Cui, J. Wang, W. Kang, C. Y. Foo and P. S. Lee, *Adv. Energy Mater.*, 2014, **4**, 1–6.

102 Z. Song, T. Ma, R. Tang, Q. Cheng, X. Wang, D. Krishnaraju, R. Panat, C. K. Chan, H. Yu and H. Jiang, *Nat. Commun.*, 2014, **5**, 1–6.

103 S. Xu, Y. Zhang, J. Cho, J. Lee, X. Huang, L. Jia, J. A. Fan, Y. Su, J. Su, H. Zhang, H. Cheng, B. Lu, C. Yu, C. Chuang, T. Il Kim, T. Song, K. Shigeta, S. Kang, C. Dagdeviren, I. Petrov, P. V. Braun, Y. Huang, U. Paik and J. A. Rogers, *Nat. Commun.*, 2013, **4**, 1543–1548.

104 K. Liu, B. Kong, W. Liu, Y. Sun, M. S. Song, J. Chen, Y. Liu, D. Lin, A. Pei and Y. Cui, *Joule*, 2018, 1–9.

105 L. Wang, Y. Zhang, J. Pan and H. Peng, *J. Mater. Chem. A*, 2016, **4**, 13419–13424.

106 C. Shi, T. Wang, X. Liao, B. Qie, P. Yang, M. Chen, X. Wang, A. Srinivasan, Q. Cheng, Q. Ye, A. C. Li, X. Chen and Y. Yang, *Energy Storage Mater.*, 2019, **17**, 136–142.

107 J. Ren, Y. Zhang, W. Bai, X. Chen, Z. Zhang, X. Fang, W. Weng, Y. Wang and H. Peng, *Angew. Chem., Int. Ed.*, 2014, **53**, 7864–7869.

108 Y. Zhang, W. Bai, J. Ren, W. Weng, H. Lin, Z. Zhang and H. Peng, *J. Mater. Chem. A*, 2014, **2**, 11054–11059.

109 Y. Zhang, W. Bai, X. Cheng, J. Ren, W. Weng, P. Chen, X. Fang, Z. Zhang, H. Peng, Y. Zhang, W. Bai, X. Cheng,

J. Ren, W. Weng, P. Chen, X. Fang, Z. Zhang and H. Peng, *Angew. Chem., Int. Ed.*, 2014, **53**, 14564–14568.

110 A. M. Zamarayeva, A. E. Ostfeld, M. Wang, J. K. Duey, I. Deckman, B. P. Lechene, G. Davies, D. A. Steingart and A. C. Arias, *Sci. Adv.*, 2017, **3**, e1602051.

111 Y. Xu, Y. Zhao, J. Ren, Y. Zhang and H. Peng, *Angew. Chem., Int. Ed.*, 2016, **55**, 7979–7982.

112 M. Kaltenbrunner, G. Kettlgruber, C. Siket, R. Schwödiauer and S. Bauer, *Adv. Mater.*, 2010, **22**, 2065–2067.

113 D. Liu, L. Su, J. Liao, B. Reeja-Jayan and C. Majidi, *Adv. Energy Mater.*, 2019, **1902798**, 1–12.

114 R. Kumar, J. Shin, L. Yin, J. M. You, Y. S. Meng and J. Wang, *Adv. Energy Mater.*, 2017, **7**, 1602096, DOI: 10.1002/aenm.201602096.

115 A. Zhou, R. Sim, Y. Luo and X. Gao, *J. Mater. Chem. A*, 2017, **5**, 21550–21559.

116 M. Gu, W.-J. Song, J. Hong, S. Y. Kim, T. J. Shin, N. A. Kotov, S. Park and B.-S. Kim, *Sci. Adv.*, 2019, **5**, eaaw1879.

117 X. Chen, H. Huang, L. Pan, T. Liu and M. Niederberger, *Adv. Mater.*, 2019, **1904648**, 1904648.

118 Blue Spark Technologies, <https://www.bluesparktechnologies.com/index.php/products-and-services/battery-products/101-blue-spark-st-standard-series2>.

119 Powerstream, <https://www.powerstream.com/thin-lithium-ion.htm>.

120 D. J. Spencer, *Knitting Technology*, Elsevier, 2001, pp. 161–170.

121 B. M. Ghadi, M. Yuan and H. Ardebili, *Extrem. Mech. Lett.*, 2019, **32**, 1–9.

122 J. Liang, S. Wang, H. Yu, X. Zhao, H. Wang, Y. Tong, Q. Tang and Y. Liu, *Sustainable Energy Fuels*, 2020, DOI: 10.1039/C9SE01120J.

123 Q. Cheng, Z. Song, T. Ma, B. B. Smith, R. Tang, H. Yu, H. Jiang and C. K. Chan, *Nano Lett.*, 2013, **13**, 4969–4974.

124 D. H. Kim, N. Lu, R. Ma, Y. S. Kim, R. H. Kim, S. Wang, J. Wu, S. M. Won, H. Tao, A. Islam, K. J. Yu, T. Il Kim, R. Chowdhury, M. Ying, L. Xu, M. Li, H. J. Chung, H. Keum, M. McCormick, P. Liu, Y. W. Zhang, F. G. Omenetto, Y. Huang, T. Coleman and J. A. Rogers, *Science*, 2011, **333**(6044), 838–843, DOI: 10.1126/science.1206157.

125 P. Albertus, S. Babinec, S. Litzelman and A. Newman, *Nat. Energy*, 2018, **3**, 16–21.

126 Z. Yu, D. G. Mackanic, W. Michaels, M. Lee, A. Pei, D. Feng, Q. Zhang, Y. Tsao, C. V. Amanchukwu, X. Yan, H. Wang, S. Chen, K. Liu, J. Kang, J. Qin, Y. Cui and Z. Bao, *Joule*, 2019, **3**, 2761–2776.

127 G. Qian, B. Zhu, X. Liao, H. Zhai, A. Srinivasan, N. J. Fritz, Q. Cheng, M. Ning, B. Qie, Y. Li, S. Yuan, J. Zhu, X. Chen and Y. Yang, *Adv. Mater.*, 2018, **30**, 1–8.

128 H. Sun, Y. Zhang, J. Zhang, X. Sun and H. Peng, *Nat. Rev. Mater.*, 2017, **2**, 1–12.

129 Y. Zhou, C. H. Wang, W. Lu and L. Dai, *Adv. Mater.*, 2019, **1902779**, 1–24.

130 J. Lee, B. Llerena Zambrano, J. Woo, K. Yoon and T. Lee, *Adv. Mater.*, 2019, **1902532**, 1–28.

131 F. Mo, G. Liang, Z. Huang, H. Li, D. Wang and C. Zhi, *Adv. Mater.*, 2019, **1902151**, 1902151.

132 Y. Xu, Y. Zhang, Z. Guo, J. Ren, Y. Wang and H. Peng, *Angew. Chem., Int. Ed.*, 2015, **54**, 15390–15394.

133 G. Liu, J. Y. Kim, M. Wang, J. Y. Woo, L. Wang, D. Zou and J. K. Lee, *Adv. Energy Mater.*, 2018, **8**, 1–9.

134 G. Berckmans, M. Messagie, J. Smekens, N. Omar, L. Vanhaverbeke and J. Van Mierlo, *Energies*, 2017, **10**(9), 1314, DOI: 10.3390/en10091314.

135 J. H. Schünemann, H. Dreger, H. Bockholt and A. Kwade, *ECS Trans.*, 2016, **73**, 153–159.

136 D. Wirthl, R. Pichler, M. Drack, G. Kettlhuber, R. Moser, R. Gerstmayr, F. Hartmann, E. Bradt, R. Kaltseis, C. M. Siket, S. E. Schausberger, S. Hild, S. Bauer and M. Kaltenbrunner, *Sci. Adv.*, 2017, **3**, 1–10.

137 Y. Ding, X. Guo, Y. Qian, L. Zhang, L. Xue, J. B. Goodenough and G. Yu, *Adv. Mater.*, 2019, **31**, 1–9.

138 X. Guo, Y. Ding, L. Xue, L. Zhang, C. Zhang, J. B. Goodenough and G. Yu, *Adv. Funct. Mater.*, 2018, **28**, 1–8.

139 X. Guo, L. Zhang, Y. Ding, J. B. Goodenough and G. Yu, *Energy Environ. Sci.*, 2019, **12**, 2605–2619.

140 Z. Tehrani, T. Korochkina, S. Govindarajan, D. J. Thomas, J. O'Mahony, J. Kettle, T. C. Claypole and D. T. Gethin, *Org. Electron.*, 2015, **26**, 386–394.

141 P. Andersson Ersman, R. Lassnig, J. Strandberg, D. Tu, V. Keshmiri, R. Forchheimer, S. Fabiano, G. Gustafsson and M. Berggren, *Nat. Commun.*, 2019, **10**, 5053.

142 J. Lopez, Y. Sun, D. G. Mackanic, M. Lee, A. M. Foudeh, M. S. Song, Y. Cui and Z. Bao, *Adv. Mater.*, 2018, **30**, 1804142.

143 Y.-Z. Zhang, Y. Wang, T. Cheng, W.-Y. Lai, H. Pang and W. Huang, *Chem. Soc. Rev.*, 2015, **44**, 5181–5199.

144 Z. Yu, L. Tetard, L. Zhai and J. Thomas, *Energy Environ. Sci.*, 2015, **8**, 702–730.

145 B. C. Kim, J.-Y. Hong, G. G. Wallace and H. S. Park, *Adv. Energy Mater.*, 2015, **5**, 1500959.

146 Y. Wang, Y. Ding, X. Guo and G. Yu, *Nano Res.*, 2019, **12**, 1978–1987.

147 S. Yao and Y. Zhu, *Adv. Mater.*, 2015, **27**, 1480–1511.

148 M. Shao, Z. Li, R. Zhang, F. Ning, M. Wei, D. G. Evans and X. Duan, *Small*, 2015, **11**, 3530–3538.

149 N. R. Chodankar, D. P. Dubal, G. S. Gund and C. D. Lokhande, *J. Energy Chem.*, 2016, **25**, 463–471.

150 L. Yao, Q. Wu, P. Zhang, J. Zhang, D. Wang, Y. Li, X. Ren, H. Mi, L. Deng and Z. Zheng, *Adv. Mater.*, 2018, **30**, 1706054.

151 X. Liu, C. Guan, Y. Hu, L. Zhang, A. M. Elshahawy and J. Wang, *Small*, 2017, **14**, 1702641.

152 G. Xiong, C. Meng, R. G. Reifenberger, P. P. Irazoqui and T. S. Fisher, *Adv. Energy Mater.*, 2013, **4**, 1300515.

153 Y. Zhao, X. He, R. Chen, Q. Liu, J. Liu, J. Yu, J. Li, H. Zhang, H. Dong, M. Zhang and J. Wang, *Chem. Eng. J.*, 2018, **352**, 29–38.

154 N. Zhang, Y. Li, J. Xu, J. Li, B. Wei, Y. Ding, I. Amorim, R. Thomas, S. M. Thalluri, Y. Liu, G. Yu and L. Liu, *ACS Nano*, 2019, **13**, 10612–10621.

155 K.-H. Choi, J. Yoo, C. K. Lee and S.-Y. Lee, *Energy Environ. Sci.*, 2016, **9**, 2812–2821.

156 L. Zhang, P. Zhu, F. Zhou, W. Zeng, H. Su, G. Li, J. Gao, R. Sun and C. Wong, *ACS Nano*, 2015, **10**, 1273–1282.

157 K. Jost, D. Stenger, C. R. Perez, J. K. McDonough, K. Lian, Y. Gogotsi and G. Dion, *Energy Environ. Sci.*, 2013, **6**, 2698.

158 L. Dong, C. Xu, Y. Li, C. Wu, B. Jiang, Q. Yang, E. Zhou, F. Kang and Q.-H. Yang, *Adv. Mater.*, 2015, **28**, 1675–1681.

159 W. Chen, R. B. Rakhi, L. Hu, X. Xie, Y. Cui and H. N. Alshareef, *Nano Lett.*, 2011, **11**, 5165–5172.

160 S. Chen, G. He, H. Hu, S. Jin, Y. Zhou, Y. He, S. He, F. Zhao and H. Hou, *Energy Environ. Sci.*, 2013, **6**, 2435.

161 C. J. Zhang, M. P. Kremer, A. Seral-Ascaso, S.-H. Park, N. McEvoy, B. Anasori, Y. Gogotsi and V. Nicolosi, *Adv. Funct. Mater.*, 2018, **28**, 1705506.

162 C. J. Zhang, B. Anasori, A. Seral-Ascaso, S.-H. Park, N. McEvoy, A. Shmeliov, G. S. Duesberg, J. N. Coleman, Y. Gogotsi and V. Nicolosi, *Adv. Mater.*, 2017, **29**, 1702678.

163 P.-Y. Chen, M. N. Hyder, D. Mackanic, N.-M. D. Courchesne, J. Qi, M. T. Klug, A. M. Belcher and P. T. Hammond, *Adv. Mater.*, 2014, **26**, 5101–5107, DOI: 10.1002/adma.201400828.

164 X. Wang, B. Liu, R. Liu, Q. Wang, X. Hou, D. Chen, R. Wang and G. Shen, *Angew. Chem.*, 2014, **126**, 1880–1884.

165 H. Park, J. W. Kim, S. Y. Hong, G. Lee, D. S. Kim, J. Oh, S. W. Jin, Y. R. Jeong, S. Y. Oh, J. Y. Yun and J. S. Ha, *Adv. Funct. Mater.*, 2018, **28**, 1707013.

166 T. Chen, L. Qiu, Z. Yang, Z. Cai, J. Ren, H. Li, H. Lin, X. Sun and H. Peng, *Angew. Chem., Int. Ed.*, 2012, **51**, 11977–11980.

167 Y. Huang, M. Zhong, F. Shi, X. Liu, Z. Tang, Y. Wang, Y. Huang, H. Hou, X. Xie and C. Zhi, *Angew. Chem., Int. Ed.*, 2017, **56**, 9141–9145.

168 Y. Huang, M. Zhong, Y. Huang, M. Zhu, Z. Pei, Z. Wang, Q. Xue, X. Xie and C. Zhi, *Nat. Commun.*, 2015, **6**, 10310, DOI: 10.1038/ncomms10310.

169 T. Gu and B. Wei, *J. Mater. Chem. A*, 2016, **4**, 12289–12295.

170 J. Yu, W. Lu, S. Pei, K. Gong, L. Wang, L. Meng, Y. Huang, J. P. Smith, K. S. Booksh, Q. Li, J.-H. Byun, Y. Oh, Y. Yan and T.-W. Chou, *ACS Nano*, 2016, **10**, 5204–5211.

171 T.-H. Chang, T. Zhang, H. Yang, K. Li, Y. Tian, J. Y. Lee and P.-Y. Chen, *ACS Nano*, 2018, **12**, 8048–8059.

172 J. Zang, C. Cao, Y. Feng, J. Liu and X. Zhao, *Sci. Rep.*, 2015, **4**, 6492, DOI: 10.1038/srep06492.

173 C. Cao, Y. Zhou, S. Ubnoske, J. Zang, Y. Cao, P. Henry, C. B. Parker and J. T. Glass, *Adv. Energy Mater.*, 2019, **9**, 1900618.

174 G. Lee, J. W. Kim, H. Park, J. Y. Lee, H. Lee, C. Song, S. W. Jin, K. Keum, C.-H. Lee and J. S. Ha, *ACS Nano*, 2018, **13**, 855–866.

175 D. Qi, Z. Liu, Y. Liu, W. R. Leow, B. Zhu, H. Yang, J. Yu, W. Wang, H. Wang, S. Yin and X. Chen, *Adv. Mater.*, 2015, **27**, 5559–5566.

176 L. Li, Z. Lou, W. Han, D. Chen, K. Jiang and G. Shen, *Adv. Mater. Technol.*, 2017, **2**, 1600282.

177 J. Pu, X. Wang, R. Xu and K. Komvopoulos, *ACS Nano*, 2016, **10**(10), 9306, DOI: 10.1021/acsnano.6b03880.

178 Z. Lv, Y. Tang, Z. Zhu, J. Wei, W. Li, H. Xia, Y. Jiang, Z. Liu, Y. Luo, X. Ge, Y. Zhang, R. Wang, W. Zhang, X. J. Loh and X. Chen, *Adv. Mater.*, 2018, **30**, 1805468.

179 S. He, J. Cao, S. Xie, J. Deng, Q. Gao, L. Qiu, J. Zhang, L. Wang, Y. Hu and H. Peng, *J. Mater. Chem. A*, 2016, **4**, 10124–10129.

180 Z. Lv, Y. Luo, Y. Tang, J. Wei, Z. Zhu, X. Zhou, W. Li, Y. Zeng, W. Zhang, Y. Zhang, D. Qi, S. Pan, X. J. Loh and X. Chen, *Adv. Mater.*, 2018, **30**, 1870008.

181 S. Jiao, A. Zhou, M. Wu and H. Hu, *Adv. Sci.*, 2019, **6**, 1900529.

182 D. Kim, G. Shin, Y. J. Kang, W. Kim and J. S. Ha, *ACS Nano*, 2013, **7**, 7975–7982.

183 Y. Lim, J. Yoon, J. Yun, D. Kim, S. Y. Hong, S.-J. Lee, G. Zi and J. S. Ha, *ACS Nano*, 2014, **8**, 11639–11650.

184 S. Y. Hong, J. Yoon, S. W. Jin, Y. Lim, S.-J. Lee, G. Zi and J. S. Ha, *ACS Nano*, 2014, **8**, 8844–8855.

185 C. Choi, J. H. Kim, H. J. Sim, J. Di, R. H. Baughman and S. J. Kim, *Adv. Energy Mater.*, 2017, **7**, 1602021, DOI: 10.1002/aenm.201602021.

186 Z. Yang, J. Deng, X. Chen, J. Ren and H. Peng, *Angew. Chem., Int. Ed.*, 2013, **52**, 13453–13457.

187 J. Yu, W. Lu, J. P. Smith, K. S. Booksh, L. Meng, Y. Huang, Q. Li, J.-H. Byun, Y. Oh and T.-W. Chou, *Adv. Energy Mater.*, 2017, **7**, 1600976, DOI: 10.1002/aenm.201600976.

188 G. Zhou, N. Kim, S. Chun, W. Lee, M. Um, T. Chou, M. F. Islam, J. Byun and Y. Oh, *Carbon*, 2018, **130**, 137–144.

189 M. Li, M. Zu, J. Yu, H. Cheng and Q. Li, *Small*, 2017, **13**, 1602994.

190 Z. Lu, J. Foroughi, C. Wang, H. Long and G. G. Wallace, *Adv. Energy Mater.*, 2017, **8**, 1702047.

191 S. Wang, N. Liu, J. Su, L. Li, F. Long, Z. Zou, X. Jiang and Y. Gao, *ACS Nano*, 2017, **11**(2), 2066, DOI: 10.1021/acsnano.6b08262.

192 H. Park, J. W. Kim, S. Y. Hong, G. Lee, H. Lee, C. Song, K. Keum, Y. R. Jeong, S. W. Jin, D. S. Kim and J. S. Ha, *ACS Nano*, 2019, **13**, 10469–10480.

193 N. Li, T. Lv, Y. Yao, H. Li, K. Liu and T. Chen, *J. Mater. Chem. A*, 2017, **5**, 3267–3273.

194 A. Lamberti, F. Clerici, M. Fontana and L. Scaltrito, *Adv. Energy Mater.*, 2016, **6**, 1600050.

195 Z. Zhang, L. Wang, Y. Li, Y. Wang, J. Zhang, G. Guan, Z. Pan, G. Zheng and H. Peng, *Adv. Energy Mater.*, 2017, **7**, 1601814.

196 X. Wang, C. Yang, J. Jin, X. Li, Q. Cheng and G. Wang, *J. Mater. Chem. A*, 2018, **6**, 4432–4442.

197 C.-R. Chen, H. Qin, H.-P. Cong and S.-H. Yu, *Adv. Mater.*, 2019, **31**, 1900573.

198 T. An, B. Zhu, Y. Ling, S. Gong and W. Cheng, *J. Mater. Chem. A*, 2019, **7**, 14233–14238.

199 L. Wang, X. Feng, L. Ren, Q. Piao, J. Zhong, Y. Wang, H. Li, Y. Chen and B. Wang, *J. Am. Chem. Soc.*, 2015, **137**, 4920–4923.

200 N. Kurra, B. Ahmed, Y. Gogotsi and H. N. Alshareef, *Adv. Energy Mater.*, 2016, **6**, 1601372.

201 T. An, Y. Ling, S. Gong, B. Zhu, Y. Zhao, D. Dong, L. W. Yap, Y. Wang and W. Cheng, *Adv. Mater. Technol.*, 2019, **4**, 1800473.

202 N. Bowden, S. Brittain, A. G. Evans, J. W. Hutchinson and G. M. Whitesides, *Nature*, 1998, **393**, 146–149.

203 Z. Niu, H. Dong, B. Zhu, J. Li, H. H. Hng, W. Zhou, X. Chen and S. Xie, *Adv. Mater.*, 2012, **25**, 1058–1064.

204 Q. Tang, M. Chen, G. Wang, H. Bao and P. Saha, *J. Power Sources*, 2015, **284**, 400–408.

205 C. Yu, C. Masarapu, J. Rong, B. Wei and H. Jiang, *Adv. Mater.*, 2009, **21**, 4793–4797.

206 Y. Zhang, Y. Huang and J. A. Rogers, *Curr. Opin. Solid State Mater. Sci.*, 2015, **19**, 190–199.

207 I. Nam, S. Bae, S. Park, Y. G. Yoo, J. M. Lee, J. W. Han and J. Yi, *Nano Energy*, 2015, **15**, 33–42.

208 I. Nam, G.-P. Kim, S. Park, J. W. Han and J. Yi, *Energy Environ. Sci.*, 2014, **7**, 1095.

209 S. He, L. Qiu, L. Wang, J. Cao, S. Xie, Q. Gao, Z. Zhang, J. Zhang, B. Wang and H. Peng, *J. Mater. Chem. A*, 2016, **4**, 14968–14973.

210 H. Guo, M.-H. Yeh, Y.-C. Lai, Y. Zi, C. Wu, Z. Wen, C. Hu and Z. L. Wang, *ACS Nano*, 2016, **10**, 10580–10588.

211 Y. Zhang, S. Wang, X. Li, J. A. Fan, S. Xu, Y. M. Song, K.-J. Choi, W.-H. Yeo, W. Lee, S. N. Nazaar, B. Lu, L. Yin, K.-C. Hwang, J. A. Rogers and Y. Huang, *Adv. Funct. Mater.*, 2013, **24**, 2028–2037.

212 L. Li, Z. Lou, D. Chen, K. Jiang, W. Han and G. Shen, *Small*, 2017, **14**, 1702829.

213 J. S. Heo, J. Eom, Y.-H. Kim and S. K. Park, *Small*, 2017, **14**, 1703034.

214 P. Li, Z. Jin, L. Peng, F. Zhao, D. Xiao, Y. Jin and G. Yu, *Adv. Mater.*, 2018, **30**, 1800124.

215 Y.-H. Lee, Y. Kim, T.-I. Lee, I. Lee, J. Shin, H. S. Lee, T.-S. Kim and J. W. Choi, *ACS Nano*, 2015, **9**, 12214–12223.

216 K. Dong, Y.-C. Wang, J. Deng, Y. Dai, S. L. Zhang, H. Zou, B. Gu, B. Sun and Z. L. Wang, *ACS Nano*, 2017, **11**, 9490–9499.

217 H. Sun, S. Xie, Y. Li, Y. Jiang, X. Sun, B. Wang and H. Peng, *Adv. Mater.*, 2016, **28**, 8431–8438.

218 C. C. Ho, K. Murata, D. A. Steingart, J. W. Evans and P. K. Wright, *J. Micromech. Microeng.*, 2009, **19**, 094013, DOI: 10.1088/0960-1317/19/9/094013.

219 L. Li, L. Pan, Z. Ma, K. Yan, W. Cheng, Y. Shi and G. Yu, *Nano Lett.*, 2018, **18**, 3322–3327.

220 C. L. Cobb and C. C. Ho, *Electrochem. Soc. Interface*, 2016, **25**, 75–78.

221 S. Gong and W. Cheng, *Adv. Energy Mater.*, 2017, **7**, 1700648.